

## **Responses to Anonymous Referee #1**

### **• Reviewer's comment:**

*This paper presents tidal proxies in MIPAS temperatures inferred as global ascending-descending node differences. The authors explain how these differences highlight diurnal and terdiurnal ("odd") harmonics, and present longitudinal spectral decompositions as a function of latitude, altitude and month. The novelty of the work lies in the presentations of MIPAS thermospheric temperatures, the first such results presented above 100 km. This paper is very pertinent to thermospheric dynamics and energetics, and should inform tidal modeling and studies of vertical coupling. I recommend publication after the comments below are addressed, and after a more thorough editing for English grammar.*

### **Author's response:**

We thank the Reviewer for his/her comments. We think we addressed them all and they certainly improved the manuscript. A native English speaker has checked the grammar of the reviewed version.

Main changes of the manuscript are: update of the version of retrieved thermospheric temperatures (results barely change); inclusion of new figures with lower altitude of 40 km; old Sect. 3 has been moved to an Appendix; the discussion on thermospheric tides has been extended.

### **• Reviewer's comment:**

1. Abstract, line 9-10: The data do not inform you of the QBO transmission process; only the facts should be reported. Change to " ...4) a quasi-biennial oscillation of the migrating tide in the stratosphere and the MLT."

### **Author's response:**

Done.

### **• Reviewer's comment:**

2. Lines 35-36: *"Tidal inter-annual variability is thought to be correlated with the El Nino-Southern Oscillation (ENSO)"*

*The following paper demonstrated clearly how ENSO causes tidal variability.*

*Lieberman, R. S., D. M. Riggan, D. A. Ortland, S. W. Nesbitt, and R. A. Vincent (2007), Variability of mesospheric diurnal tides and tropospheric diurnal heating during 1997–1998, J. Geophys. Res., 112, D20110, doi:10.1029/2007JD008578.*

### **Author's response:**

We deleted 'thought to be' and included the reference.

### **• Reviewer's comment:**

3. Lines 47-48: *"The extent to which tides propagate from the lower atmosphere to the thermosphere or to which changes in lower altitude regions are transmitted by tides to the upper atmosphere or to other latitudes is not completely known."*

*The following papers should be cited in this section:*

*Talaat, E. R., and R. S. Lieberman (2010), Direct observations of nonmigrating diurnal tides in the equatorial thermosphere, Geophys. Res. Lett., 37, L04803, doi:10.1029/2009GL041845.*

*Lieberman, R. S., J. Oberheide, and E. R. Talaat (2013), Nonmigrating diurnal tides observed in global thermospheric winds, J. Geophys. Res. Space Physics, 118, 7384– 7397, doi:10.1002/2013JA018975.*

Lieberman, R. S., D. M. Riggan, D. A. Ortland, J. Oberheide, and D. E. Siskind (2015), *Global observations and modeling of nonmigrating diurnal tides generated by tide-planetary wave interactions*, *J. Geophys. Res. Atmos.*, 120, doi:10.1002/2015JD023739.

**Author's response:**

Done. They are now included in the next paragraph of the manuscript.

• **Reviewer's comment:**

4. Lines 58-70. *This paragraph is extremely confusing, and should be deleted. The authors discuss sun-synchronous sampling before the MIPAS satellite and its orbit are even mentioned. Non-sun-synchronous sampling is not relevant here.*

**Author's response:**

An unavoidable caveat in sun-synchronous measurements is aliasing of certain tidal modes. Slowly precessing satellites eventually provide a complete local time coverage that overcomes that problem but at the expense of the temporal resolution. We did not delete the whole paragraph in the text but we significantly shorten and clarify it. We have also exchanged the order of this paragraph and the (old) next one.

• **Reviewer's comment:**

5. Lines 74-76: *"Therefore, they provide a wealth of information on the tidal excitation mechanisms, the processes inducing tidal variability and the lower and upper atmosphere coupling through tides". Delete this statement. The data cannot accomplish all of that on their own, only in combination with models.*

**Author's response:**

We think that the study of correlations among measured longitudinal oscillations and also with external sources help to understand excitation mechanisms (Immel et al., 2006; Xu et al., 2014), atmospheric coupling (Oberheide and Forbes, 2008; Forbes et al., 2009) and variability processes (Zhang and Shepherd, 2005; Forbes et al., 2008).

Nevertheless, we agree that this information must be demonstrated in combination with models. Therefore, we softened the sentence by substituting 'provide a wealth of information' by 'may reveal indications'.

• **Reviewer's comment:**

6. Section 3, beginning. *I suggest preceeding line 134 with a BRIEF qualitative discussion of the consequences of sun-synchronous sampling. E. g., "Because MIPAS observations occur at 2 fixed local times, migrating tides (that depend only on local time) are seen as invariant features over the course of a day... We explore this and other ramifications of MIPAS sampling in the following discussion..."*

**Author's response:**

Following the suggestion from the other referee, we have moved Section 3 to an Appendix. The new Appendix has been also modified. Nevertheless, we included the sentence suggested by the referee in Sect. 3.1.

• **Reviewer's comment:**

7. Line 134: *Sentence needs clarification: "An atmospheric variable  $X$  consisting only of tides and a background state at altitude  $z$ , latitude, longitude and Universal Time (UT)  $\hat{A}^{\sim}$  can be expressed as the sum of the background zonal mean value and the sum of all individual tidal components  $X_{n,s}$  with zonal wavenumber  $s$  and wave frequency  $n$  at that position and time.."*

**Author's response:**

We have slightly changed the sentence and shortened the paragraph.

• **Reviewer's comment:**

8. Line 168: Delete "solution".

**Author's response:**

Done.

• **Reviewer's comment:**

9. Lines 183-188: Delete.

**Author's response:**

We have almost deleted the complete paragraph but have left the reference.

• **Reviewer's comment:**

10. Line 204-205. Change to "an oscillation tilting eastward with height..."

**Author's response:**

Done.

• **Reviewer's comment:**

11. Lines 208-209: Change to "Fig. 1 exhibits wave features tilting westward with height (18 km vertical wavelength)..."

**Author's response:**

Done.

• **Reviewer's comment:**

12. Lines 211-212: "This feature is difficult to notice..." Delete. In general, do not dwell on things that are not in the data.

**Author's response:**

It is true that this is not a striking feature in Fig. 1 in October but, as it is shown later (Fig.10), it certainly is in the data. It is weak and masked by other oscillations in Fig. 1. We substituted 'difficult to notice' by 'perceived (...) but it is not as evident as at lower altitudes or in August,'.

• **Reviewer's comment:**

13. Line 237: Delete "mainly".

**Author's response:**

Done.

• **Reviewer's comment:**

14. Lines 239-240: "including the information of the local time phase." This will confuse the reader, suggest deleting.

**Author's response:**

Done. (We moved the sentence suggested by the reviewer some comments above to this paragraph).

• **Reviewer's comment:**

15. Line 254: Chapman and Lindzen predicted a vertical wavelength of 27 km for (1,1). Please specify where the observed vertical wavelength of "20-30 km" is smaller or larger than C & L's predictions.

**Author's response:**

Done.

• **Reviewer's comment:**

16. Line 305: Change to "...and the zonal winds in the middle atmosphere.."

**Author's response:**

Done.

• **Reviewer's comment:**

17. Line 330: Change to "They may originate..." and reference previously mentioned Lieberman et al., 2015. paper.

**Author's response:**

Done.

• **Reviewer's comment:**

18. Lines 334-335: "The monotonical change in phase with altitude..." I suggest selecting 3 key latitudes -equatorial, and midlatitude northern and southern hemisphere - and generating line plots of the phase with altitude. That would make it much easier to see the phase tilt.

**Author's response:**

This is a great suggestion. We now include two new figures: new Figs. 7 and 10.

• **Reviewer's comment:**

19. Lines 340-344: "Those features probably belong..." Delete.

**Author's response:**

Done.

• **Reviewer's comment:**

20. Line 372: "MIPAS |nodd -s|=2 longitudinal oscillation embeds the diurnal DE1 and DW3 and the terdiurnal TW1 and TW2 components..."

No mention of TW2 is made in Table 1 for MIPAS wave 2, and the math I use (based on Salby's formulas) yields an alias of 1 for TW2.

**Author's response:**

As correctly pointed out by the referee, TW2 yields 1, as shown in Table 1. TW2 deleted in the text.

• **Reviewer's comment:**

21. Lines 373-374: "...both are most likely originated by non-linear interactions between their migrating counterpart (DW1 and TW3, respectively) and the  $s = 1$  stationary planetary wave (SPW1)."

The verbiage here is very muddy. What do you mean by "both"? DE1 and DW3?

What are you proposing for the interactions? DW1 + SPW1, and TW3 + SPW1? Neither one of these produces DE1, DW3, TW1 or TW2.

**Author's response:**

That sentence was definitely wrong. These non-migrating tides could originate from non-linear interactions between their migrating counterparts (DW1 and TW3) and  $s=2$  stationary planetary waves (SPW2). Changed.

• **Reviewer's comment:**

22. Lines 375-376 ("Not many tidal analyses..."): Delete.

**Author's response:**

Re-written.

**• Reviewer's comment:**

23. Lines 406-407: "The phase dependence with altitude indicates contribution from an eastward propagating wave..." Again, show line plots at representative latitudes. It is actually quite difficult to determine phase tilt in contour plots. Also, the phase appears to be increasing with height in the southern hemisphere, and decreasing with height in the northern hemisphere.

**Author's response:**

Thank you again for this suggestion. As mentioned above, we now include Fig. 10 showing the phase tilt with height.

**• Reviewer's comment:**

Line 409: "Amplitudes from 115-150 km during December also exhibit eastward propagation."

Do you mean to say here that the phases increase with altitude???

**Author's response:**

Yes, we did mean that phases increase with altitude. Re-written.

**• Reviewer's comment:**

24. Line 432: Replace monotonically with "increasing".

**Author's response:**

Done. Sentence re-written.

**• Reviewer's comment:**

25. Lines 437-438: "...phase moves westward as latitude increases... phase moves eastward..." Use phrases such as "phase increases/decreases with latitude".

**Author's response:**

Done.

**• Reviewer's comment:**

26. Lines 487-488: "The DE3 component should also present a QBO (Li et al., 2015) but small and it is not surprising that we could not detect it in MIPAS data." Delete.

**Author's response:**

We re-phrased the sentence.

**• Reviewer's comment:**

27. Lines 520-524: "That suggest then that the effect on tides..." Delete these lines.

**Author's response:**

We think that, assuming the argument from Ekanayake et al., (1997) (stronger tides when direction of propagation is opposite to the wind), if the QBO effect on the migrating tide (westward propagation) were produced locally in the mesosphere, the tide amplitude would strengthen when the zonal wind mesospheric QBO were in its westerly phase (wind towards the east). That is *not* the case in MIPAS data. The tide, on the contrary, strengthens during the westerly phase of the stratospheric QBO. Therefore, it is *more likely* that the tide QBO originates in the stratosphere. The later is however not necessarily true and that is why we leave a door open and write in Sect. 4 (old Sect. 5) that other mechanisms cannot be ruled out.

We think this reasoning is not a speculation but suggests that the mesospheric tide QBO is not a local effect.

Nevertheless, we re-wrote the paragraph and say that MIPAS suggests that a stratospheric effect is more likely than a mesospheric effect. We hope that the argument is clearer now and eludes speculations.

• **Reviewer's comment:**

28. *Figure 13: Convert to a line only at altitude of amplitude maximum.*

**Author's response:**

We think that substituting this color map by a 1D plot with amplitude vs. latitude at only one selected altitude would eliminate a lot of information. We believe the figure is simple and clear enough. We think that all information on the dependence of the amplitude on altitude and latitude can easily be shown with this map. Additionally, Fig. 14 (old Fig.12) gives some more information at the latitude where the QBO peaks.

• **Reviewer's comment:**

29. *Line 549: Delete "as expected".*

**Author's response:**

Done

• **Reviewer's comment:**

30. *Lines 576-577: "Comparison of tidal QBO and zonal wind stratospheric..." Delete.*

**Author's response:**

Changed to: 'the effect on tides does not mainly occur in the mesosphere' (see argument in response to comment 27).

• **Reviewer's comment:**

*In general the figures were much too small for a review copy.*

**Author's response:**

We re-did all figures. We hope they meet the standards of ACP.

• **Reviewer's comment:**

1. *Figure 1: Use monthname-day-year format rather than yyyyymmdd in the Figure titles.*

**Author's response:**

Done.

• **Reviewer's comment:**

2. *I suggest either enlarging the latitude-altitude plots, or starting them at  $z = 60$  km. Since the amplitudes are very weak below 60 km, most of these plots are empty space, and they squish the more interesting behavior at high altitudes into too small of a space.*

**Author's response:**

We moved the Figures up to 40 km. We note that Zeng et al. (2008) detected DW1 activity (although with very small amplitudes 1K) already in the lower stratosphere.

***References (used in this document but not included in the manuscript)***

Forbes, J.; M.; Zhang, X.; Palo, S.; Russell, J.; Mertens, C.; J. & Mlynczak, M. Tidal variability in the ionospheric dynamo region, *Journal of Geophysical Research*, **2008**, 113, A02310 .

Oberheide, J.; Forbes, J.M. Tidal propagation of deep tropical cloud signatures into the thermosphere from TIMED observations, *Geophys. Res. Lett.*, **2008**, *35*, L04816.

Xu, J.; Smith, A. K.; Liu, M.; Liu, X.; Gao, H.; Jiang, G.; Yuan, W. Evidence for nonmigrating tides produced by the interaction between tides and stationary planetary waves in the stratosphere and lower mesosphere, *J. Geophys. Res.*, **2014**, *119*, 471-489.

Zhang, S.; P.; Shepherd, G. G. Variations of the mean winds and diurnal tides in the mesosphere and lower thermosphere observed by WINDII from 1992 to 1996 *Geophys. Res. Lett.*, **2005**, *32*, L14111.

Zeng, Z., W. Randel, S. Sokolovskiy, C. Deser, Y.-H. Kuo, M. Hagan, J. Du, and W. Ward (2008), Detection of migrating diurnal tide in the tropical upper troposphere and lower stratosphere using the Challenging Minisatellite Payload radio occultation data, *J. Geophys. Res.*, *113*, D03102, doi:10.1029/2007JD008725.

### **Anonymous Referee #3**

#### **• Reviewer's comment:**

*The manuscript aims to diagnose migrating and nonmigrating tides in 5-year monthly mean averages of MIPAS/ENVISAT temperature observations between 20-150 km and 80S-80N. The Sun-synchronous ENVISAT orbit prevents a standard Fourier analysis due to the lacking local solar time coverage. Instead, the manuscript uses the well-known ascending-descending orbit differencing technique to obtain amplitudes and phases of the zonal wavenumber 0-4 patterns in the satellite local solar time frame. The inherent limitation of the approach is that it does not allow one to separate between diurnal and terdiurnal signals, and westward and eastward propagating nonmigrating tidal components. The observed zonally symmetric pattern, that is, the superposition of the migrating diurnal and terdiurnal tides, is also analyzed on a monthly basis (w/o the 5-year averaging) and compared to the stratospheric Singapore zonal winds, in order to derive a QBO modulation amplitude. Comparisons with the migrating diurnal tide from the GSWM tidal model and NRLMSISE-00 are also shown.*

*Any new information about tidal characteristics in the 110-150 km region is of value to the aeronomy community since global tidal observations in the transition region into the diffusive regime, where tidal amplitudes and phase are constant with height, are very sparse. As such, I believe the manuscript should ultimately be published. There are, however, a number of important shortcomings in the manuscript that impact its scientific impact.*

#### **Author's response:**

We thank the referee for his/her very useful comments that we think have improved the manuscript. We have taken into account his/her suggestions.

Main changes of the manuscript are: update of the version of retrieved thermospheric temperatures (results barely change); inclusion of new figures with lower altitude of 40 km; old Sect. 3 has been moved to an Appendix; introduction and discussion on thermospheric tides has been extended.

#### **• Reviewer's comment:**

*1. The meat of the manuscript are the data above 110 km since temperature tides in the MLT and below have already been extensively analyzed on monthly mean tides using SABER and MLS data. SABER diagnostics can actually separate tidal components in the MLT and MIPAS does not contribute much here. The bottom line of the lengthy description of MIPAS MLT tidal characteristics in section 4 is that it agrees with SABER. It thus should be scaled back significantly and the paper should focus on the new contribution from MIPAS, that is, tides above 110 km.*

#### **Author's response:**

MIPAS, MLS and SABER are different instruments on different platforms. We think measurements of all three of them (and other instruments) are equally interesting and, thus, it is worth reporting them all.

MIPAS and SABER results qualitatively agree, a result itself, but they do not coincide. As explained several times in the manuscript, temporal resolution of SABER standard analyses is worse than that of MIPAS (2 months vs. 1 month).

Opposite to SABER, that yaws every two months to observe the two poles alternatively, MIPAS provides a pole-to-pole view of the MLT. In this context, the effect of the mesospheric migrating tide measured at high latitudes simultaneously in both hemispheres can be reported here. Also, high latitude tide activity can be tracked along the year by MIPAS ( $k=1,4$ ).

Compared to MLS, MIPAS vertical resolution, that affects wave structures (see Sect. 2), is better.

Finally, MIPAS offers the rare opportunity to observe the atmosphere from the stratosphere up to 150 km globally. Since tides generally propagate from low altitudes, a continuous vertical coverage from a single instrument is an advantage, as we mention in the abstract and in Sect. 1.

Nevertheless, following the referee's suggestion, we tried to shorten the text deleting several full paragraphs on the discussion below 110km in Sect. 3, particularly, in its introduction and Sections 3.1 and 3.2 but also in Sect. 3.5.

**• Reviewer's comment:**

*For example, an interesting finding is the occurrence of the secondary  $k=4$  amplitude maximum above 130 km in Figure 9. This certainly warrants more discussion. I also believe the higher peak altitude of the  $k=4$  pattern warrants more discussion. From a modeling point of view, it is very difficult to shift the maximum towards higher altitudes. This would require a substantial change in the dissipation scheme, resulting in much higher tidal amplitudes in the upper thermosphere. This would then lead to breaking the currently very good agreement with CHAMP and GRACE DE3 tidal diagnostics. In addition, Figure 12 of Lieberman et al. (2013, doi:10.1002/2013JA018975) indicates that the tidal dissipation schemes are actually quite good when comparing to WINDII, including the height of the amplitude maximum. A higher altitude of the DE3 tidal temperature maximum -which would also change the vertical wavelength- would also be difficult to reconcile with DE3 observations above 110 in infrared emissions observed by SABER, since the latter are driven by temperature. See Oberheide et al. (2013, doi:10.1002/2013JA019278). More discussion of possible reasons for the inconsistency between MIPAS, the current empirical tidal models (and thus also with observed tidal winds from WINDII and infrared emissions from SABER) is needed.*

**Author's response:**

We appreciate this comment. We do not actually see such a disagreement with models, as the referee mentions. Amplitudes over the equator increase with altitude from the upper mesosphere to 120-125 km, where they reach its maximum in the altitude range examined in this work. This qualitatively agrees with the results for temperature from models, that place the DE3 peak around 110-115 km (see Sect. 3.5 for references). The 10 km shift might be partially explained by the large vertical resolution of MIPAS temperatures in the thermosphere. We note that, as pointed by the referee, the peak in the  $u$  and  $v$  fields are placed around 105 km. We have included a broader discussion on the  $k=4$  peak altitude in Sect. 3.5.

**• Reviewer's comment:**

*2. There is a considerable number of migrating tide - QBO studies in the MLT from SABER, and it is difficult to see what is new in MIPAS. Everything agrees with SABER. I am OK with leaving section 5 as it is but the earlier work by Huang et al. should be given credit.*

**Author's response:**

Done.

**• Reviewer's comment:**

*3. Tides above 110 km react very strongly to solar conditions, mainly due to the temperature dependence of thermal conductivity. The key figures in the manuscript are 5-year monthly mean averages, from 2007 to 2012, and as such do not account for the*

*important solar cycle dependence. The current results only show that tides are present, but this is something the community already knows. What's needed here is to do the diagnostics for individual years because this would actually help modelers to better constrain dissipative processes and help with our physical understanding of tidal characteristics in the thermosphere.*

**Author's response:**

We agree that analysis of individual years providing information on influence of solar conditions would be of great interest. There are several reasons why we think it is not adequate to perform such analysis from MIPAS data. Firstly, continuous observations should extend for a big portion of the solar cycle or, at least, for a portion for which changes in solar flux are important. Unfortunately, that is not the case for MIPAS data. The data cover solar flux changes of the order of 50 sfu. Maximum variations from 2007 to 2012 of monthly 10AM DW1 temperature contributions at 150km in NRLMSISE-00 are 4-7K (depending on season). Secondly, not only DW1 amplitudes vary with the solar cycle but also phases and those would be tracked in MIPAS locked LT measurements together with the solar cycle impact. Thirdly, regarding other significant modes in the thermosphere, variations along the solar cycle in the altitude range studied here are expected to be hardly detectable (see Fig.4 for DE3 in Oberheide et al., 2009)

We note that, even if the community already knows that the tides are present, a quantitative analysis, even from averages, is valuable. We focus our comparisons with SABER because it has provided reliable measurements of tides and they have been used as input for several models. We additionally recall that temperature tide measurements in the E-region are scarce and those covering from the stratosphere up to that region from a single instrument inexistent.

**• Reviewer's comment:**

4. The manuscript does not demonstrate a broad knowledge of previous work in the field. Global tidal observations in the thermosphere are sparse, but the authors seem to be unaware of a number of studies based on WINDII and SABER. See for example Talaat and Lieberman (2010, doi:1029/2009GL041845), Lieberman et al. (2013, doi:10.1002/2013JA018975), Cho and Shepherd (2015, doi:10.1002/2015JA021903), Oberheide et al. (2013, doi:1002/2013JA019278), and other. I grant that these studies deal with tides in winds and infrared emissions but they have been conclusively connected to in-situ tidal temperature diagnostics from CHAMP and GRACE in the upper thermosphere (see the various papers by Jeff Forbes) using empirical tidal modeling, including the abovementioned solar cycle dependence.

**Author's response:**

We have included a number of new references along the text and tried to put our results into their context (particularly in the introduction but also along Section 3).

**• Reviewer's comment:**

*I also believe the presented results need to be put more carefully into the context of recent progress in whole atmosphere modeling, e.g., using WACCM-X, WAM, and GAIA. The current discussion in the GCM context is essentially limited to a one year long run of the CMAM model that has been done a few years ago. CMAM development has been stopped a few years ago and more up-to-date models (or at the very least the more recent eCMAM30 run) are more appropriate for this discussion.*

**Author's response:**

The aim of this paper is to report and describe MIPAS measurements of tides in the context of previous measurements but not to perform a thorough comparison with models. That will be the focus of future work, for which taking into account MIPAS sampling and vertical resolution is needed. Nevertheless, in this new version of the manuscript, we tried to put our results in the context of several models, particularly in Sect. 3.1 and also in Sect. 3.5, when discussing the peak altitude disagreement.

We note that we only mention CMAM in order to identify DE1 as the main contributor of  $k=2$  but do not perform a direct comparison with CMAM.

• **Reviewer's comment:**

*5. What is the purpose of the GSWM/MSIS comparisons? What model version has been used and how? The given GSWM reference points to an old TIME-GCM study (where GSWM was used as a lower boundary condition only). There are several versions of GSWM around, the most recent one is GSWM-09 (see papers by Xiaoli Zhang). I doubt that this one has been used since no reference is given. Older GSWM versions had issues with seasonal variations and partly did not include the in-situ tidal forcing in the thermosphere. Also, GSWM is for 110 sfu (if I remember correctly) and does not include any solar flux dependence.*

**Author's response:**

The purpose is twofold: to see how well MIPAS ascending-descending zonal means ( $k=0$  mode; DW1+TW3) compare with 10AM-10PM migrating tide fields in models and to evaluate how the migrating tides in the a priori are transferred to MIPAS temperatures (the a priori acts as a vertically smoothing agent through the Tikhonov constraint in our retrievals). After this referee's comment, we understand that it is confusing to use two models for comparison. For consistency, we now only compare with one model at all altitudes. We chose MSIS, the a priori. The averaging kernels already pointed out that MIPAS thermospheric temperature measurement have a good quality (see Bermejo-Pantaleón et al., 2011), but the comparison presented here further supports that the retrieved temperatures do not contain significant information on model vertical structures. The comparison however shows a poor agreement between the measurements and the model. We have re-written the discussion accordingly.

We will postpone a thorough comparison with other models (not only GSWM) for a future work. Nevertheless, following another comment of this referee suggesting discussion in the context of models, we kept in the text the comparison with GSWM and also other models. We note that we now updated the GSWM results to GSWM-09 (Zhang et al., 2010a; Zhang et al., 2010b).

• **Reviewer's comment:**

*I am also puzzled to see that MSIS shows such a poor agreement with MIPAS. The MSIS amplitudes close to 150 km look way too small for migrating tides. Forbes et al. (2011, doi:10.1029/2011JA016855) compare the MSIS migrating diurnal tide at 400 km with CHAMP and GRACE. The agreement is actually quite good with amplitudes on the order of 120 K.*

**Author's response:**

We note that in the comparisons we have taken into account MIPAS sampling. MIPAS measurements provide the contribution of the DW1+TW3 only at 10AM. This coincides with the total migrating tide amplitude (which is the one shown in Forbes et al.) only at

the altitudes where the phase is 10AM. That is not the case of altitudes above 130km, where the in-situ diurnal tide, with a phase at 2-4PM in MSISE data, dominates. According to MSISE and as shown in the plot, DW1 contribution at 10AM is 15K at 150km (compared to 30K total MSISE DW1 amplitude).

We already mentioned this caveat in the text. We even wrote the factor of underestimation of the total DW1 amplitude. Nevertheless, we have re-written that paragraph for clarification.

• **Reviewer's comment:**

*6. Several conclusions are not supported by the data and speculation. (1) How do you know the propagation direction from the latitude/height Figure 7 (section 4.3, section 6)? Longitude/height plots give some indication about propagation direction, assuming that all tidal signals are propagating upward w/o any possible downward propagation or in-situ forcing (which is an assumption that needs to be stated!).*

**Author's response:**

We agree. We only know the tilt of the phase with altitude at certain latitude in the latitude/height maps of the phase (right hand side plots). The assumption of a vertical direction of propagation for proposing certain horizontal direction of propagation is now stated in the text in the introduction of Sect. 3 and also when used (several times along the manuscript). Following a suggestion of Referee#1, we now also include two figures where we plot the phase vs. altitude at selected latitudes (new Figs. 7 and 10). We hope this point is clearer in the manuscript now.

• **Reviewer's comment:**

*(2) The TW3 as the leading migrating component at 110 km (section 4.1, section 6) is mere speculation since MIPAS cannot separate DW1 and TW3. In-situ DW1 forcing is as likely (or more likely).*

**Author's response:**

We now make stress in section 4.1 and section 6 that DW1 is as likely.

• **Reviewer's comment:**

*7. Methodology section 3. I doubt that a non-expert in tidal satellite diagnostics will understand this section. It gives an overly complicated description of a well-established method that has been applied over the past 20 years to every single remote sensing infrared instrument when looking into tides. I strongly suggest to significantly shorten the section (or moving the shortened version into section 2 altogether). If the authors insist to keep this level of detail, the section should be moved into an appendix, but with the addition of a few intermediate steps that have been omitted, to help readers not familiar with the satellite orbit geometries and sampling.*

**Author's response:**

We moved old Section 3 to an Appendix. We have also re-written the section with the hope that it is more easily readable now.

Specific comments.

• **Reviewer's comment:**

*line 523. Oberheide et al. (2009) do not discuss the QBO in the westward propagating migrating tide, only in the eastward propagating DE3.*

**Author's response:**

We re-wrote the sentences and say now that Oberheide et al.'s referred to DE3.

• **Reviewer's comment:**

*The lower altitude in the Figures should be moved up to 50 or 70 km. There's not much tidal activity going on in the stratosphere.*

**Author's response:**

We moved lowest altitude of the Figures up to 40 km. We note that Zeng et al. (2008) detected DW1 activity (although with very small amplitudes 1K) already in the lower stratosphere.

• **Reviewer's comment:**

*The language is mostly fine but another round of proof-reading by the native speaker on the co-author list would be good.*

**Author's response:**

A native English speaker has proof-read the text.

**References**

Oberheide, J., M. G. Mlynczak, C. N. Mosso, B. M. Schroeder, B. Funke, and A. Maute (2013), Impact of tropospheric tides on the nitric oxide 5.3 um infrared cooling of the low-latitude thermosphere during solar minimum conditions, *J. Geophys. Res. Space Physics*, 118, 7283–7293, doi:10.1002/2013JA019278.

Oberheide, J., J. M. Forbes, X. Zhang, and S. L. Bruinsma  
Climatology of upward propagating diurnal and semidiurnal tides in the thermosphere  
*J. Geophys. Res.*, 116, A11306, doi:10.1029/2011JA016784, 2011.

Zeng, Z., W. Randel, S. Sokolovskiy, C. Deser, Y.-H. Kuo, M. Hagan, J. Du, and W. Ward (2008), Detection of migrating diurnal tide in the tropical upper troposphere and lower stratosphere using the Challenging Minisatellite Payload radio occultation data, *J. Geophys. Res.*, 113, D03102, doi:10.1029/2007JD008725.

# MIPAS observations of longitudinal oscillations in the mesosphere and the lower thermosphere: Climatology of odd-parity daily frequency modes

Maya García-Comas<sup>1</sup>, Francisco González-Galindo<sup>1</sup>, Bernd Funke<sup>1</sup>, Angela Gardini<sup>1</sup>, Aythami Jurado-Navarro<sup>1</sup>, Manuel López-Puertas<sup>1</sup>, and William E. Ward<sup>2</sup>

<sup>1</sup>Instituto de Astrofísica de Andalucía-CSIC, Granada, Spain

<sup>2</sup>Department of Physics, University of New Brunswick, Fredericton, New Brunswick, Canada

*Correspondence to:* Maya García-Comas  
Instituto de Astrofísica de Andalucía-CSIC  
Glorieta de la Astronomía s/n  
18008 Granada, Spain (maya@iaa.es)

**Abstract.** MIPAS global sun-synchronous observations are almost ~~locked~~ fixed in local time. Subtraction of the descending and ascending node measurements at each longitude only ~~contain~~ includes the longitudinal oscillations with odd daily frequencies  $n_{odd}$  from ~~a solar~~ the Sun's perspective at 10 A.M. Contributions ~~of from~~ the background atmosphere, ~~persistent (on a daily basis) longitudinal oscillations~~ daily-invariant zonal oscillations and tidal modes with ~~even~~ even-parity daily frequencies vanish.

5 We have determined ~~MIPAS temperature longitudinal oscillations~~ longitudinal oscillations in MIPAS temperature with  $n_{odd}$  and wavenumber  $k=0-4$  from ~~20 the stratosphere~~ to 150 km from April 2007 to March 2012. To our knowledge, this is the first time ~~temperature zonal oscillations are derived~~ zonal oscillations in temperature have been derived pole-to-pole in this altitude range ~~globally~~ from a single instrument. The major findings are the detection of: 1) migrating tides at Northern and Southern high latitudes; 2) significant  $k = 1$  activity at extra-tropical and high-latitudes, particularly in the SH; 3)  $k = 3$  and

10  $k = 4$  eastward propagating waves that penetrate ~~in~~ the lower thermosphere with a significantly larger vertical wavelength than in the mesosphere; 4) a migrating tide quasi-biennial ~~oscillation of the migrating tide mainly originated~~ oscillation in the stratosphere ~~and propagated to the MLT, mesosphere and lower thermosphere~~. MIPAS global measurements of longitudinal oscillations are useful for testing tide modeling in the MLT region and as a lower boundary ~~of for~~ models extending higher up in the atmosphere.

## 15 1 Introduction

One of the most prominent and ~~persistent dynamical features in~~ enduring dynamic features of the mesosphere and ~~the~~ lower thermosphere (MLT) are the atmospheric solar tides (referred ~~as simply to as~~ tides hereafter). They are oscillations with periods that are subharmonics of a solar day. ~~Particular cases among them are~~ A case in point is that of the migrating tides, which are westward propagating oscillations with a phase speed equal to the Earth's angular velocity,  $\Omega$ . ~~They apparently travel~~ They

20 give the appearance of travelling with the Sun, ~~and depend on the solar local~~ dependent on the local solar time (LST) but not

on longitude. Migrating tides are excited by a longitude independent source, such as the absorption of solar IR radiation by water vapor in the troposphere, the solar UV radiation absorption by ozone in the stratosphere, and the local solar UV and EUV radiation absorption by oxygen molecules and atoms, respectively, and ~~maybe also possibly by~~ chemical heating (Smith et al., 2003), in the thermosphere.

25 The non-migrating tides also have periods which are subharmonics of a solar day but may be either westward or eastward propagating, or stationary and their phase speed is ~~different from not~~  $\Omega$ . They are excited by longitudinally varying properties, like tropospheric latent heat release from evaporation, ~~Sun gravitational pullor the sun's gravitational pull~~, heating rates, ~~and by nonlinear and by non-linear~~ wave-wave interactions. An interaction between zonal wavenumber  $s$  asymmetries in surface or atmospheric properties and the absorption of the  $n^{th}$  harmonic of the diurnally varying solar radiation generates a sum and  
30 a difference tide with frequency  $n\Omega$  and zonal wavenumbers  $n \pm s$ . For example, the zonally asymmetric latent heat release in the tropical troposphere caused by the wavenumber-4 land-sea distribution modulates the migrating diurnal DW1 component to excite the DE3 and DW5 tidal pair (Hagan and Forbes, 2002; Zhang et al., 2006). As an example of wave-wave interactions, involving tides and planetary waves, the interaction of the stationary planetary wave-1 sPW1 with DW1 leads to the formation of D0 and DW2 tidal modes (~~Hagan and Roble, 2001~~). (~~Hagan and Roble, 2001; Mayr et al., 2005a; Lieberman et al., 2015~~).  
35 Note that the widely used 3-character notation for tides is also used here. The first letter corresponds to the daily frequency (D corresponds to diurnal; S corresponds to semidiurnal; T corresponds to terdiurnal). The second letter indicates the direction of propagation (W for westward and E for eastward). The number is the absolute value of the tide zonal wavenumber.

Tides also interact with other ~~dynamical processes. waves~~. Tidal inter-annual variability is ~~thought to be~~ correlated with the El Nino-Southern Oscillation (ENSO) (~~Gurubaran et al., 2005~~) (~~Gurubaran et al., 2005; Lieberman et al., 2007~~) and the wind  
40 Quasi-Biennial Oscillation (QBO) (~~McLandress, 2002; Mayr and Mengel, 2005~~) (~~McLandress, 2002; Mayr and Mengel, 2005; Xu et al., 2005~~) planetary and gravity wave (GW) activity may affect tidal activity (~~Fritts and Vincent, 1987; Teitelbaum and Vial, 1991; Pedatella and Liu, 2002~~) (~~Fritts and Vincent, 1987; Teitelbaum and Vial, 1991; Mayr et al., 2005b; Pedatella and Liu, 2012; Ribstein et al., 2015~~); GW and tidal non-linear interaction significantly affects winds (Liu et al., 2014). Nevertheless, there is no complete understanding of how these processes take place. For example, it is not clear if the mesospheric QBO signature originates at stratospheric  
45 levels, locally in the mesosphere or both (Oberheide et al., 2009).

~~Tides generally~~ ~~Tides often~~ propagate upwards. ~~Despite~~ ~~Regardless of~~ the location of its source, the amplitude of upward propagating tides ~~grows with altitude due to the conservation of energy in a density decreasing with altitude environment. The tides originated at the troposphere that increases with altitude, due to energy conservation in an environment of decreasing-with-altitude density.~~

50 ~~The tides that originate in the troposphere and~~ propagate vertically connect the lower, ~~the middle and the middle and~~ upper atmospheres. They also produce a second order impact on atmospheric vertical coupling as they modulate the upward propagation of other waves, like gravity waves (Eckermann and Marks, 1996; Senf and Achatz, 2011). The connection also extends in the latitudinal direction because tides become a global feature under its standing wave latitudinal structure.

~~The~~ ~~Over the last two decades, much progress has been made on determining the~~ extent to which tides propagate from  
55 the lower atmosphere to the ~~thermosphere or to which~~ ~~ionosphere;~~ or changes in lower altitude regions are transmitted by

tides to the upper atmosphere or to other latitudes ~~is not completely known. The 100-150km range is a region of particular~~  
~~, but this knowledge is still incomplete. In this context, the lower thermosphere, in particular, the E-region, is of inter-~~  
est. Vertically-propagating tides maximize at those altitudes, where molecular dissipation dominates (Forbes and Garrett,  
1979). They impact the spatial and temporal variability through electrodynamical effects, ~~that and~~ are transmitted even higher  
60 ~~(Kil et al., 2007; Hagan et al., 2007; Jin et al., 2008). The temperature tidal spectrum at these altitudes is not well known~~ (Immel et al., 2006)

Several authors have studied tides from satellite measurements in this altitude region in recent years. The analyses are based  
on observations of wind fields (Oberheide and Forbes, 2008a; Talaat and Lieberman, 2010; Lieberman et al., 2013; Cho and Shepherd, 2011),  
atmospheric species emission rates or abundances (Oberheide and Forbes, 2008b; Shepherd, 2011; Oberheide et al., 2013; Nee, 2014, see e.g.,  
65 ~~the ionized atmosphere~~ (England et al., 2006; Chu et al., 2009; Mukhtarov and Pancheva, 2011, see e.g., ). Few global obser-  
vations of the neutral atmosphere are available ~~there. TIMED measurements covered altitudes in the 100-150 km altitude range.~~  
Temperatures have generally been analyzed at the lowest altitudes of this range (generally below 115 km ~~(see e.g., Xu et al., 2009; Pancheva~~  
~~CHAMP above 400)~~ using TIMED, Aura or WINDII satellite measurements (see e.g., Wang et al., 2000; Forbes and Wu, 2006; Xu et al., 2006,  
70 ~~or above the range, using WINDII measurements around 250 km (Shepherd et al., 2012) and CHAMP measurements of the~~  
~~exosphere (Forbes et al., 2008; Oberheide et al., 2009; Bruinsma and Forbes, 2010; Forbes et al., 2014, see e.g., ). Studies of~~  
~~longitudinal oscillations measured by MIPAS on Envisat for this altitude range have been conducted by (Xu et al., 2013) but~~  
~~only for selected atmospheric conditions (aurorae). The global temperature tidal spectrum is therefore not very well known at~~  
~~100-150 km (Forbes et al., 2008; Oberheide et al., 2009; Bruinsma and Forbes, 2010; Forbes et al., 2014, see e.g., ). Besides the~~  
~~knowledge of the . Besides understanding the~~ local behavior, ~~observations at 100-150km observations at these altitudes~~ are  
75 needed to discern the origin of longitudinal oscillations higher up in the atmosphere. Characterizing the non-migrating ~~tides~~  
~~is relevant even only in the lowest altitudes of this range , as a temperature tides there is relevant as this range constitutes the~~  
lower boundary in numerical models.

~~The analysis of tides from atmospheric measurements is generally complicated. Ideally, the latitudinal, longitudinal and~~  
~~local time coverage should be complete to isolate the tidal components contributing to the observed signal. The absence of~~  
80 ~~longitudinal coverage of ground-based instrumentation results in strong tidal aliasing. Analogously, sun-synchronous satellite~~  
~~instrumentation (with two fixed local times of observations 12 hours apart) does not provide a good local time coverage~~  
~~but, in contrast to ground-based instruments, it allows for tidal observations on a global scale. Besides, the combination of the~~  
~~measurements taken at these two fixed times cancels out particular tidal frequencies and reduces aliasing, as we do in this work.~~  
~~Non sun-synchronous instruments certainly allow for the separation of individual tidal components (Zhang et al., 2006; Gan et al., 2014; Tr~~  
85 ~~However, their slow preceeding period requires grouping measurements covering periods larger than months in order to~~  
~~achieve a complete local time coverage and, thus, the temporal resolution is degraded. Isolation of the tidal components with~~  
~~a finer time resolution can be achieved only if two tidal components with daily frequency of different parity contribute to~~  
~~an observed longitudinal wavenumber in the local time frame (Li et al., 2015) . Thus, as we will show here, the advantage~~  
~~of sun-synchronous instruments is their ability to better resolve longitudinal oscillations globally at high time resolution,~~  
90 ~~particularly, where more than two daily frequencies contribute.~~

The Michelson Interferometer for Passive Atmospheric Sounding (MIPAS) (Fischer et al., 2008) measured the Earth ~~temperature globally from pole to pole~~'s temperature from pole to pole, covering altitudes from 20 to ~~150~~170 km ~~onboard~~ on board a sun-synchronous satellite, Envisat. ~~Observations of temperature longitudinal oscillations with~~, offering the rare opportunity to observe longitudinal oscillations globally in this altitude range from a single instrument. MIPAS wide spatial (~~both horizontal and vertical~~) and temporal coverage ~~and temporal coverages~~ are ideal for constraining ~~tide~~ tidal vertical and latitudinal extent and global variations in seasonal and inter-annual ~~timescales~~. ~~Therefore, they provide a wealth of information on time scales~~. Additionally, they may reveal indicators for the tidal excitation mechanisms, the processes inducing tidal variability and the lower and upper atmosphere coupling through tides. Additionally, the characterization of the tides in an atmospheric measurement dataset is a prerequisite ~~to estimate~~ for estimating trends (Beig et al., 2003).

The analysis of tides from atmospheric measurements is complex. Ideally, a complete longitudinal and local time coverage is needed in order to isolate the tidal components contributing to the observed signal. Sun-synchronous observations at 12 hour intervals at fixed local times, like MIPAS, do not provide good local time coverage but the combination of the measurements made in each node reduces aliasing (Oberheide et al., 2002; Lieberman et al., 2015). Non-sun-synchronous observations allow for the separation of individual tidal components but the slow satellite precession period generally worsens the temporal resolution (e.g. Zhang et al., 2006; Gan et al., 2014; Truskowski et al., 2014).

This work describes the ~~MLT temperature longitudinal oscillations~~ longitudinal oscillations in temperature measured by MIPAS ~~during five full years from 40 to 150 km over a five year period (March 2007-March 2012)~~. ~~Inspired by its~~ With the benefit of the sun-synchronous observational strategy, we extract the longitudinal wavenumbers as ~~would be~~ viewed by an observer ~~sitting on the Sun with the ability to isolate daily frequency parities. We divided the work in two parts: this paper covers the observed odd daily frequency temperature components and a companion paper focuses on the even daily frequency oscillations (García-Comas et al., 2015)~~, capable of isolating daily parities. This paper describes the observed temperature oscillations with odd-parity daily frequencies.

~~This~~ The paper is organized as follows. Section 2 describes the MIPAS temperature observations used in this work. ~~Section A presents the method used to extract longitudinal oscillations from a longitudinal series of observations. The monthly~~ Monthly climatologies of the observed longitudinal wavenumbers are presented in ~~Seet~~ Section 3, where we discuss their latitude, altitude and seasonal behavior in the context of other measurements. Section 4 includes a description of the inter-annual variability of the main oscillations. We ~~close up~~ end with a summary of the main findings. Appendix A includes a description of the method used.

## 2 The instrument, data set and error sources

MIPAS measurements ~~are distributed over the full globe~~ have full global coverage and were taken ~~during~~ for the descending and ~~the~~ ascending nodes at approximately two fixed local times, 10 A.M. and 10 P.M., respectively (in general, local times differ from the average values by less than half an hour at latitudes equatorward of 75° and by three quarters of an hour equatorward of 85°). The MIPAS Middle Atmosphere (MA) and ~~the~~ Upper Atmosphere (UA) modes of observation resulted in an altitude

coverage of 18–102 km and 40–170 km, respectively (Oelhaf, 2008). While operating with ~~optimized-resolution-optimized~~  
125 ~~resolution~~ (0.0625 cm<sup>-1</sup>; unapodized), full day observations using these modes were performed regularly (approximately one  
day in each mode every 10 days) from April 2007 to March 2012, thus covering five ~~complete years.~~ ~~years.~~

MIPAS spectra ~~covered-range~~ from 4.3 to 15.6  $\mu\text{m}$ . Temperature and line of sight information (LOS) are derived in the MLT  
region from the 15  $\mu\text{m}$  CO<sub>2</sub> emission using the IMK/IAA scientific MIPAS level 2 processor described in von Clarmann et al.  
(2009), which accounts for non-LTE effects using the GRANADA model (Funke et al., 2012). ~~We use in this work~~ ~~In this study~~  
130 ~~we use~~ data versions V5R\_TLOS\_521 and V5R\_TLOS\_621 of MA and UA, respectively, retrievals (García-Comas et al.,  
2014), which provide temperature profiles with ~~a vertical resolution of~~ 3 to 10 km ~~vertical resolution,~~ from the stratosphere up  
to around 110 km ( $T_{MLT}$ ) (García-Comas et al., 2012).

Thermospheric temperatures ( $T_{THER}$ ) from 115 km up to 150 km are derived from MIPAS 5.3  $\mu\text{m}$  NO emission measure-  
ments in the UA mode (~~Bermejo-Pantaleón et al., 2011~~) ~~with a 5–10~~ ~~with a vertical resolution of 10–15 km~~ ~~vertical resolution~~  
135 ~~At the time of writing this paper, a single data version covering the 2007–2012 period is not yet available. We therefore~~  
~~use two retrieval versions, V4O(2007–2009) and~~ km (Bermejo-Pantaleón et al., 2011) . ~~We use retrieval version~~ V5R\_TT\_621  
~~(2010–2012)~~ of  $T_{THER}$ . ~~These two data versions differ mainly in~~ ~~This version differs from that described in Bermejo-Pantaleón et al. (2011)~~  
the spectra calibration version supplied by ESA. ~~Bermejo-Pantaleón et al. (2011) found that their derived nighttime temperatures~~  
~~(V4O) might be affected by artifacts. The new data version V5R corrects this problem by using~~ ~~and in the use of~~ NOEM day  
140 and night concentrations (Marsh et al., 2004) as *a priori*, ~~that correct artifacts affecting night-time temperatures.~~ Tests showed  
that ~~the new~~ ~~this~~ temperature version leads to similar ~~structures of the day/night zonal mean differences~~ ~~night-time zonal mean~~  
~~temperature structures~~ but smaller in absolute value by 10–15K below 140 km and 15–25K above 140 km. ~~It is important noting~~  
~~that, even if the day/night temperature differences retrieved from these versions do not differ, their longitudinal anomalies are~~  
~~similar (amplitude differences smaller than 5K). Thus, combination of these two versions is reasonable, in particular, for the~~  
145 ~~study of non-migrating components.~~

~~Despite~~ MIPAS temperature systematic errors ~~are significant~~ (1–3K below 85 km and 3–10K above 85 km) ~~for~~  $T_{MLT}$ , and  
10–20K for  $T_{THER}$ ), ~~we analyze here~~ ~~but as we analyze~~ differences of longitudinal perturbations about an average value  
(see Sect. A). ~~Thus~~, biases often partially cancel out so that their effect on the derived ~~oscillations~~ ~~oscillation~~ characteristics  
are small. Additionally, we work with monthly averages, which reduce the random error by at least a factor of  $1/\sqrt{3}$ . One  
150 of the most significant errors we expect is that produced by the limited vertical resolution. At the peaks of a vertical wave,  
the wave amplitude error due to that smoothing  ~~$A_{smoo}$  can be estimated with:~~ where  ~~$A$  is the wave amplitude,~~  ~~$\lambda_z$  is the~~  
~~wave vertical wavelength, and  $\Delta z$  is the vertical resolution.~~ ~~As an example, MIPAS Tsmoothing error for a 10~~ ~~depends on its~~  
~~vertical wavelength. Smoothing errors are 2–5% in the mesosphere, 15% around 120 km and 30% around 140 km for 25 km~~  
vertical wavelength ~~wave is 15% whereas for a 30~~ ~~waves. They increase for short vertical wavelengths, reaching 15–30% in the~~  
155 ~~mesosphere and 60% around 120 km for 10 km vertical wavelength~~ ~~wave the error is 2%.~~ ~~waves.~~

The temperature retrieval algorithm uses *a priori* information of the temperature at each MIPAS geolocation taken from  
ECMWF at pressures larger than 0.1 hPa ( ~~$\approx 70$  km~~) and merged with NRLMSISE-00 model results at lower pressures.  
NRLMSISE-00 includes only effects of low order tides (Picone et al., 2002). ~~In order to detect any potential impact of~~

~~We examined *a priori* zonal oscillations on the retrieved temperatures, we examined NRLMSISE-00 temperature variations~~  
160 ~~temperature oscillations~~ with longitude in the fixed local time frame of MIPAS. ~~A migrating component most likely corresponding~~  
~~to DW1 is present in the model, with the largest perturbations in the equinoxes and over the equator and alternating minima and~~  
~~maxima at 55km, 70km, 95km and 110km. Out of phase weaker oscillations appear only at 60° North and South at 70–75km.~~  
~~Another maximum appears above 145km, displaced 20–30° off the equator in the summer, that is, following the sub-solar~~  
~~point. We only~~ Besides the migrating component, we only detect wavenumber 1 and 2 non-migrating zonal oscillations with  
165 amplitudes generally smaller than 1K. Some exceptions occur in the winter high latitudes, probably corresponding to plan-  
etary wave activity (wavenumber-1 structures reaching 10K at 40 km, 5K at 50 km and 2K at 75 km). Given the differences  
between measurement and *a priori* tidal component fields (see Sect. 3), we conclude that the mapping of *a priori* longitudinal  
oscillations on the retrievals is not significant and does not influence MIPAS temperatures.

### 3 Five-year average zonal oscillations

170 Following the procedure described in Appendix A, we derived amplitudes and phases of the longitudinal oscillations of  
apparent wavenumber  $k$  from the stratosphere to the lower thermosphere as seen in MIPAS temperature differences of the  
descending and the ascending nodes.

We have constructed longitude-altitude maps of monthly  $T_{MLT}$  and  $T_{THER}$  temperatures averaged from April 2007 to  
March 2012 for the descending and the ascending legs. In order to achieve a good longitudinal coverage with a small loss  
175 of horizontal resolution, we ~~have~~ used longitude and latitude running-means at each altitude in a  $5^\circ \times 5^\circ$  grid. At each grid  
point, we ~~have~~ averaged MIPAS monthly measurements taken within  $25^\circ$  in longitude and  $10^\circ$  in latitude bins. We ~~have~~ then  
subtracted and divided by 2 the descending and the ascending node measurements at each grid point,  $\Delta T/2$  hereafter.

Figure 1 left panels show typical  $\Delta T/2$  fields. They are August and October monthly means averaged over the five years and  
constructed from  $T_{MLT}$  and  $T_{THER}$  measurements over the equator. A background with alternating positive and negative hor-  
180 izontal stripes is evident. A longitude-independent signature at each altitude must be responsible for that pattern. A longitude-  
independent feature in  $\Delta T/2$  corresponds to a migrating component. The pattern is stronger during October (equinox) than  
August (solstice). Vertically alternating  $\Delta T/2$  maxima and minima correspond to altitudes where the tidal phase is at 10 A.M.  
(45, 75, 95 and 110 km) and 10 P.M. (60, 85 105 and 120 km), respectively. A different regime takes place above 125 km, where  
a background positive  $\Delta T/2$  remains nearly constant with altitude. That implies a nearly constant-with-altitude LST phase,  
185 that is, the oscillation does not propagate vertically. This is typical of an *in situ* generated oscillation.

The right panels in Fig. 1 are  $\Delta T/2$  longitudinal anomalies (zonal mean subtracted at each altitude) averaged for August and  
October. They contain only  $n - odd$  non-migrating tidal modes ( $|n_{odd} - s|$  larger than 0). In August, ~~an eastward propagating~~  
~~oscillation with wavenumber 4~~ a wavenumber-4 oscillation tilting eastward with height is noticeable from the mid-mesosphere  
to the thermosphere with increasing amplitude up to 130 km. A subtle underlying wave-1 perturbation propagates to the west  
190 in the upper mesosphere but suffers efficient dissipation in the lowermost part of the thermosphere.

The October  $\Delta T/2$  anomaly field in Fig. 1 exhibits ~~a vertically wavenumber-1 features tilting westward with height~~ (18 km vertical wavelength) ~~and westward propagating wavenumber-1 feature~~. This signature is noticeable from 40 km, in the stratosphere, and extends to 110 km, in the lower thermosphere. Its vertical and longitudinal structure is similar to the one in August but the October feature is significantly stronger. Starting at 105 km, a zonal wavenumber-4 structure overlaps. This feature is ~~difficult to notice~~ ~~perceived~~ on the  $T_{THER}$  fields above 115 km ~~but it is not as evident as at lower altitudes or in August~~, probably because it is weak ~~and/or~~ ~~and~~ another component overlaps.

~~Using the method described in the previous section, we have analyzed~~ ~~We performed the spectral analysis of~~ MIPAS  $\Delta T/2$  fields ~~, analogous to the ones analogous to those~~ shown in Fig. 1 ~~, at each latitude globally~~ and for the twelve months of the calendar year (see Appendix A). For each altitude  $z$ , ~~we have performed a spectral analysis to derive the amplitudes  $C_k(z, \phi)$  and phases  $\theta_k(z, \phi)$  embedding the latitude  $\phi$  and month, we derived amplitudes  $C_k$  and phases  $\theta_k$ , for which  $k$  are the apparent longitudinal wavenumbers in  $\Delta T/2$  that embed the combination of the tidal modes with odd-parity daily frequency  $n$  and zonal wavenumber  $s$  such that  $|n - s| = k$ . We hereafter denote this combined oscillation as  $|n_{odd} - s| = k$  (see Table 1 ~~summarizes the major tidal components contributing to each apparent zonal wavenumber~~.~~

~~Positive and negative wavenumbers, indicating horizontal direction of propagation, cannot be separated in the spectra. Nevertheless, if the direction of vertical propagation is known, the dependence of the phases  $\theta_k$  on altitude ultimately helps discern dominance of a particular tidal mode. For instance, assuming upward propagation, a  $\theta_k$  moving to the east (west) with increasing altitude corresponds to an eastward (westward) propagating tidal oscillation if  $s = n - k < 0$  ( $s = n + k > 0$ ).~~

Figure 2 shows the derived average amplitude spectra during equinox months (April and October) and solstice months (January and July) at 88 and 110 km from wavenumber 0 to 4. The dominance of some modes is evident and depends on season and altitude.

For latitudes within ~~45° North and South~~ ~~N and 45° S~~, the  $|n_{odd} - s| = 0$  mode is the strongest component in the upper mesosphere and below 100 km during April (and also February, March, May and August; not shown). Its amplitude ranges from 9 to 18K. The  $|n_{odd} - s| = 1$  and  $|n_{odd} - s| = 4$  oscillations follow in importance ~~in April~~. During January and October (and also September, November and December; not shown), wavenumber  $|n_{odd} - s| = 1$  is the dominating component of the tidal field (8-15K) in the mesosphere. In July (and June; not shown), wavenumber  $|n_{odd} - s| = 4$  is the most important (8K), although  $|n_{odd} - s| = 0, 1$  have similar amplitudes. MIPAS also detects  $|n_{odd} - s| = 0, 1$  oscillations around 60-70° during the summers with 2K amplitudes.

In the lower thermosphere, around 110 km, the strongest  $n - odd$  longitudinal oscillation in MIPAS data is  $|n_{odd} - s| = 0$  at latitudes smaller than 70° and also  $|n_{odd} - s| = 4$  at latitudes smaller than 40° (see Fig. 2). This happens throughout the year, the former peaking around 25° N and S (15-20K) (except during June and July) and the latter over the equator (8-16K). In July and August, the  $|n_{odd} - s| = 4$  oscillation stands out particularly and wavenumber  $|n_{odd} - s| = 1$  (15K) is then also noticeable at 25°. ~~At At the~~ highest latitudes,  $|n_{odd} - s| = 1$  is the only significant mode, although signatures from  $|n_{odd} - s| = 2$  oscillations are also present, for example, in January (12K).

Next, we ~~describe in detail~~ ~~five a detailed description of~~ each of the extracted longitudinal oscillation modes and their seasonal variations. ~~The~~ MIPAS Sun-synchronous view provides a fixed local time shot of longitudinal variations. If otherwise

not indicated, we use a phase defined in terms of longitude (positive towards the East of Greenwich) of maximum at 10 A.M. The caveat is that, ~~in our case,~~ the phase is undefined for longitudinally-standing tidal components ( $s = 0$ ).

### 3.1 The $|n_{odd} - s|=0$ mode

The  $|n_{odd} - s|=0$  mode, which is just the  $\Delta T/2$  zonal mean, contains ~~contribution mainly contributions~~ from the diurnal (DW1) and terdiurnal (TW3) migrating tides. Figures 3-5 include representative latitude-altitude and latitude-time cross sections. ~~We recall that, given MIPAS local time sampling, the values shown correspond to~~ Because MIPAS observations occur at two fixed local times, contribution from migrating tides (that depend only on local time) are seen as invariant features over longitude. The values measured correspond to the temperature perturbations produced by these migrating tides at 10 A.M., ~~including the information of the local time phase~~. These do not directly correspond to tidal amplitudes at altitudes where the vertical profiles do not peak.

~~Temperature perturbation maps at 10 A.M. for DW1 from the Global Scale Wave Model (GSWM) (Hagan and Roble, 2001) at 20-110 km and P.M. temperature difference maps for DW1 and TW3 from NRLMSISE-00 at 115-150 km and ECMWF at altitudes below around 0.1 km-mb and NRLMSISE-00 above (used as a priori, see Sect. 2) are also shown for reference. GSWM results have been comparison in Fig. 3. The model results map MIPAS LT sampling and were convolved considering MIPAS temperature vertical resolution. Note that the contribution from TW3 should be added to the GSWM model amplitudes for a direct comparison with MIPAS = 0. Yue et al. (2013), Pancheva et al. (2013) and Moudden and Forbes (2013) report up to 4K TW3 amplitudes at 90km in February and September at the equator, and 10K at 110km at the equator in January and at 50° in the equinoxes and June.~~

MIPAS  $|n_{odd} - s|=0$  latitude-altitude cross-section ~~for October exhibits maximum and minimum~~ below 120 km exhibits maximum absolute values over the equator and at ~~35° North and South N and 35° S in October~~ (Fig. 3). ~~The peaks~~ Peaks of alternating sign are located at the equator ~~are located~~ at 42 km (1K), 56 km (-1K), 74 km (5K), 84 km (-11K), 94 km (7K), 104 km (-6K), 110 km (12K) and 120 km (-20K). Out-of-phase peaks (opposite sign) occur at 35° below 105 km. Their altitudes in the Northern Hemisphere (NH) are similar to those at the equator but they are 2 km higher in the Southern Hemisphere (SH). These extra-tropical perturbations are weaker (<1K below 80 km and 2K at 84 km, -6K at 94 km, 4K at 104 km and 15K at 110 km) than ~~in at~~ the equator. ~~The~~

The a priori migrating component also presents the largest perturbations for the equinoxes and over the equator (Fig. 3). The alternating minima and maxima are located at similar altitudes below 70 km (corresponding to ECMWF) but the vertical wavelength above (NRLMSISE-00) increases and peaks are located only at 95 km and 110 km. Out of phase weaker oscillations appear only at 60° N and 60° S at 70-75 km. Global Scale Wave Model (GSWM-09; Hagan and Roble (2001); Zhang et al. (2010a, b)) and Climatological Tidal Model of the Thermosphere (CTMT; Oberheide and Forbes (2008a); Oberheide et al. (2011b)) DW1 sampled at MIPAS LT (not shown) present peaks located generally within 2-4 km and 1-2K of those of MIPAS below 100 km, except for the maxima at 70 km and 95 km over the equator (5-8K smaller in MIPAS).

MIPAS oscillation exhibits a vertical wavelength decreasing with altitude vertical wavelength of 20-30, varying from 30 km below around the stratopause to 20 km around 110 km, slightly smaller than the values associated with. This is comparable to

260 27 km, the classical tidal theory (Chapman and Lindzen, 1970) prediction for (1,1) (Chapman and Lindzen, 1970). The model DW1 has a slightly longer vertical wavelength on average than that given by MIPAS, particularly in the upper mesosphere. This could indicate caveats in the representation of gravity wave and tide interactions in this version of the model (Achatz et al., 2008). We note however that superposition of TW3 may affect the MIPAS-derived vertical wavelength.

The latitudinal structure of the phase ~~is different at altitudes changes~~ above 105 km. The perturbations from the tropics to 50°  
265 around 110 km, peaking at 35° (15K), are not out of phase with respect to the equator (they have the same sign at all latitudes). This behavior those at the equator. This is consistent with ~~a strong overlapping contribution from overlapping of~~ TW3, with the most pronounced amplitudes at mid-latitudes above 100 km ~~(Moudden and Forbes, 2013). (Moudden and Forbes, 2013; Yue et al., 2013), and/or the effect of the thermospheric in situ DW1 tide. This MIPAS feature is similar in the NRLMSISE-00 model but does not compare well with GSWM-09 or CTMT DW1 at 110 km, which exhibit typical (1,1) mode structure.~~

270 ~~The sign of the temperature perturbation at At 120 km shifts to negative, MIPAS zonal mean temperature differences switch to negative values for latitudes between 50°S and 30°N. This behavior could be explained in several ways. The negative values at this altitude accompanying the positive ones at~~ There are several possibilities that might explain this feature. It could be due mainly to TW3. If related to a feature at 110 km ~~could come from the same component, explained by TW3. That contribution, it would imply a TW3 vertical wavelength of 20 km. This is~~ larger than expected from models (Du and Ward, 2010) but similar to  
275 ~~those TW3 wavelengths~~ derived from previous measurements in the upper mesosphere (Thayaparan, 1997). Another possibility is a preferential dissipation of the low order DW1 modes from the Hough Mode Extension (HME) (Forbes and Hagan, 1982) at lower altitudes so that higher order modes dominate at these higher altitudes, ~~resulting in a different =0 latitudinal distribution. It~~. Finally, it could also be ~~the a~~ consequence of the thermospheric *in situ* DW1, ~~independent to the classical upward propagating DW1 present at altitudes below. That. The latter~~ would imply a downward propagation of the thermospheric component, ~~which could be possible allowed~~  
280 under the thermosphere viscid regime (Forbes and Garrett, 1976).

Corresponding GSWM DW1 maxima and minima in October are located within 2-4 ~~The feature at 120 km and 1-2K below 100km, except the maxima at 70km and 95km over the equator, which are 5-8K smaller in MIPAS. MIPAS and GSWM is not identifiable in GSWM-09 and CTMT DW1 fields above 100km do not compare that well. The altitude and vertical width of the MIPAS minimum around 105-110km at the equator are different in the GSWM model. This might be partially explained~~  
285 ~~by the overlapping positive TW3 contribution peaking at 110km and extending to 50°S-50°N. The measured oscillation at 110 and 115km is however similar to that centered at 115km in the results at MIPAS LT sampling. Neither in NRLMSISE-00 model, being positive at all latitudes. The model DW1 has a slightly longer vertical wavelength on average than that of =0, particularly in the upper mesosphere. This maybe indicates caveats in the representation of gravity wave and tide interactions in this version of the model (Achatz et al., 2008). nor the thermosphere extension of the Whole Atmosphere Community~~  
290 Climate Model (WACCM-X) (Liu et al., 2010), which include *in situ* DW1. We cannot rule out that part of this disagreement is due to remaining artifacts in MIPAS  $T_{THER}$  due to unrealistic *a priori* NO day/night abundances used in the retrievals (see Bermejo-Pantaleón et al. (2011)).

Comparison with 10At 130-150 km, MIPAS measures positive A.M.-10P.M. zonal mean perturbations from the NRLMSISE-00 model, used as a priori (see Sect differences at 35°S-25°N in October (Fig. 2) shows little agreement with MIPAS = 0. This strengthens the idea of the a priori having small impact on the derived temperature oscillations.

3). The nearly constant-with-altitude feature values above 130 km in Fig. 3 evidences no change in local time phase evidence no phase change with altitude. This is consistent with the effect of the thermospheric *in situ* generated tide. MIPAS measurements occur at LST=10. diurnal migrating component. The phase of the thermospheric *in situ* generated diurnal migrating component occurs at thermospheric tide is  $\varphi_{DW1}=2-4$  P.M., depending dependent on the solar flux input (Forbes and Garrett, 1976). It is then likely that amplitudes (see e.g. Forbes and Garrett, 1976; Liu et al., 2010). Since MIPAS measurements correspond to LST=10, we note that MIPAS measurements of the thermosphere DW1 tides measured by MIPAS underestimate total amplitudes, with effect underestimate total *in situ* tide amplitudes by a factor of attenuation as large as  $\cos(n\Omega(10 - \varphi_{DW1}))$ . MIPAS measures maximum amplitudes of 50K at 140-150km in October.

During April (not shown), MIPAS = 0 perturbations are 2-5K larger than in October over the equator. Opposite to results from GSWM-DW1, the peak altitudes over the equator and in the NH are slightly higher (2km) than in October. This may reflect a change of (local time) phase of the longitudinal oscillation behind. As in October, the strength of the oscillation in April is latitudinally symmetric, except around 94km (2K stronger in the NH). MIPAS perturbations in April over the equator at 84km and at 35° Comparison with the NRLMSISE-00 model shows little agreement at these altitudes. On the one hand, this strengthens the idea of the a priori having little impact on the derived temperature oscillations but, on the other hand, MIPAS significantly overestimates the model predictions. Again, artifacts in MIPAS  $T_{THER}$  below 100km are larger by 5K and 2K, respectively, than in GSWM-DW1. retrieval cannot be ruled out.

Figure 3 also shows  $|n_{odd} - s|=0$  longitudinal perturbations for January. Maximum and minimum values occur at the same altitudes as in April and are over the equator and in the NH are slightly higher (2 km) and 2-3K smaller than during in October below 110 km at low to mid-latitudes. April values are larger than those of the GSWM model. In the thermosphere, the behavior is similar to that during the rest of the year. Negative negative perturbations at 120 km are 5K stronger than in October. Above 130 km, the signature of the *in situ* tide is clear (+10-60K 10-50K), producing maximum perturbations off the equator and tracking the sub-solar point.

At Southern high latitudes (55-75°S), MIPAS sees an oscillation with peaks peaking at 90 and 100 km in January at Southern high latitudes (55-75°S) (Fig. 3). It is in phase with the perturbations at 35°, probably indicating that it belongs to a different HME mode. Its dependence with season is shown in the time series at 75°S and 70°N depicted in Fig. 4. A vertical perturbation peaking at 10 A.M. with alternating maxima and minima at 90, 100 and 110 km is clearly seen from late Spring through Summer at 75°S (2K). This structure is also present at Northern high latitudes (70°N) at similar altitudes but with slightly weaker amplitudes. This detection corroborates previous measurements of temperature tides at Southern high latitudes, where 3K amplitude diurnal components with 10 A.M. phases were measured from ground around 90 km (Lübken et al., 2011). We detect here Here we detect a Northern hemisphere counterpart.

Latitude-time slices at altitudes where  $|n_{odd} - s|=0$  generally peak (84, 110, 120 and 140 km) are shown in Figure 5. The seasonal and latitudinal variability strongly depends is highly dependent on altitude. Starting with 84 km, the perturbation

is stronger during the equinoxes than during solstices. This ~~could be~~ is due to the influence of the seasonal variation of the symmetry of the heating source (Forbes et al., 2001) ~~but more likely of and~~ the zonal winds in the middle atmosphere (McLandress, 2002; Zhu et al., 2005), probably below 70 km (Achatz et al., 2008). ~~The latitude of the maximum perturbations is slightly shifted towards the equator during July (as in GSWM DW1; not shown). The inter-hemispheric difference around 35° is generally due to a difference in the altitude of the peaks (see Sect. 4). There is an isolated minimum (-2K) around 50°N during June-July, with a weaker SH counterpart, with a significantly smaller amplitude in the model. The amplitude is smaller.~~ Amplitudes are smaller than 1K for latitudes larger than 70° at this altitude.

At 110 km, the perturbation is positive all year round, except ~~at all latitudes northern to north of 70°N, and varies significantly (2-15K).~~ Maxima are generally reached at 35°, with a 5° shift towards ~~the South in January and towards the North in July (i.e., shifted to higher latitudes in the local summer), coinciding with previously.~~ Previously detected TW3 ~~shifts (Pancheva et al., 2013). Maximum values at these latitudes occur during latitude shifts (Pancheva et al., 2013) and the in situ DW1 evidence the same behavior. Maximum values occur in~~ the equinoxes, coinciding with the expected maximum contribution from an overlapping DW1. ~~At the equator, opposite to the GSWM DW1 results, perturbations are positive. The amplitude changes significantly throughout the year (2-16K) with maximum values in July. Overlapping TW3, which presents significant reduction of amplitude at 110km right~~ Perturbations are significantly reduced over the equator during January ~~(Pancheva et al., 2013), is the most likely responsible of this behavior., as a TW3 effect would be (Pancheva et al., 2013).~~

At 120 km, MIPAS  $|n_{odd} - s|=0$  is negative between 50°S and 50°N. These negative perturbations generally peak at the same altitude along throughout the year, which implies that the local time phase ~~remains also constant.~~ also remains constant. The latitudinal structure could correspond to a second-order symmetric mode of DW1 and/or ~~and~~ the first TW3 mode. Maximum perturbations occur during ~~the~~ solstices around 20° South and North (~~-25K-20K~~), in contrast to the mesosphere, where maximum amplitudes are found at the equator during ~~the~~ equinoxes.

At 140 km, the positive peaks, following the sub-solar point, move towards the local summer, when they present maximum amplitudes. The ~~seasonal and latitudinal behavior of~~ similarities of the  $|n_{odd} - s|=0$  seasonal and latitudinal structure around 120 km ~~presents similarities to with~~ that at 140 km, ~~which could support~~ supports the possibility of ~~the~~ downward propagation of the *in situ* thermospheric DW1. ~~Negative peaks are measured during the~~ Additionally, MIPAS measurements show negative peaks at 140 km in Autumn around 50° North and South (10-15KN and 50°S (10K). These could be associated ~~to~~ with the positive perturbation at lower altitudes (120 km) ~~at~~ for similar latitudes.

### 3.2 The $|n_{odd} - s|=1$ mode

The strongest tidal modes included in the MIPAS  $|n_{odd} - s|=1$  longitudinal oscillation are DW2 and D0. TE2 and TW4 oscillations are also embedded if present. The diurnal modes are the strongest among them. They ~~probably may~~ originate from a combination of DW1 interaction with sPW1 and the longitudinally varying tropospheric latent heat release related with the wave-1 surface longitudinal asymmetry ~~(Oberheide et al., 2005)~~ (Oberheide et al., 2005; Lieberman et al., 2015).

Figure 6 shows  $n_{odd-s}=1$  amplitudes and phases derived for November. Amplitudes maximize around the equator,  $35^{\circ}\text{N}$  and  $35^{\circ}\text{S}$ , and range from 1-2K from 40 to 65 km, 2-5K from 65 to 75 km (4-15K). SH amplitudes are larger than in the NH. The extra-tropical oscillations are out of phase with those at the equator. The decreasing phase with altitude (right upper plot of Fig. 7) indicates a westward propagation. That suggest if vertical propagation is assumed. That indicates a contribution from DW2. The vertical wavelength is 25 km.

$n_{odd-s}=1$  presents significant extra-tropical activity, with amplitudes peaking also around  $35^{\circ}\text{S}$  (8K at 90km and 10K at 105km) and  $35^{\circ}\text{N}$  (4K at 90km). The SH amplitudes are thus larger. The phase also increases with altitude towards the West. The oscillation at these latitudes is out of phase with respect to that at the equator.

A hint of significantly activity with smaller amplitudes (2K at 90 km and 6K at 105 km) appears also over at  $65^{\circ}\text{S}$ . These features probably belong to the same tidal mode because they are in phase and anti-phase with the signals measured at  $0^{\circ}$  and  $35^{\circ}$ , respectively, and also show westward propagation and also tilt westward with altitude. An analogous signature appears at  $65^{\circ}\text{N}$  but its propagation direction is not as coherent.

It is not clear evident from MIPAS data how efficiently this oscillation penetrates higher up in the thermosphere. At the very least, it does not magnify as altitude increases increase with altitude in the 115-150 km range because the Tfields for this mode do. This mode does not show a coherent structure and amplitudes usually oscillate around temperature error values at these altitudes.

Figure 6 also shows time series of the amplitudes and phases of the MIPAS  $|n_{odd-s}=1$  longitudinal oscillation. Amplitudes at 68, 86 and 105 km. The amplitude at 68 km is maximum in July and November (5K) maximize in July, November and February (3K-5K). These maxima shift in latitude from  $20^{\circ}\text{N}$  in January to  $20^{\circ}\text{S}$  in July, i.e., towards the following the tropical local winter. This off-equator displacement generally occurs at altitudes between 60 and 80 km. It is also present in SABER measurements and is reproduced in CMAM30 (Gan et al., 2014). Its phase displaces from  $100^{\circ}\text{E}$  in January to  $200^{\circ}\text{E}$  in July. (Gan et al., 2014). Secondary maxima ( $<2\text{K}$ ) appear in July and November  $20-30^{\circ}$  to the North and to the South of the primary maximum.

The MIPAS  $n_{odd-s}=1$  wave amplitude at 86 km is maximum (typical  $|n_{odd-s}=1$  peaking altitude) peaks at the equator in during the equinoxes (10-15K) but also peaks in July (8K) (Fig. 6). These values are larger than the combination of those reconstructed from ISAMS measurements for DW2 (4K) and D0 (3K) (Forbes and Wu, 2006) or from SABER September 2004 DW2 (2K) and D0 (4K) (Zhang et al., 2006). The typical peaking altitude in MIPAS data below 100 km is 86 km. The phase remains constant throughout the year except in July, when it shifts  $180^{\circ}$ . This reflects a change in the relative importance of the sources of the underlying tides, which is expected to be stronger greater in July if tide-wave interaction dominates (see Fig. 3 in Oberheide et al., 2005).

The amplitude of  $|n_{odd-s}=1$  at 86 km reaches 4K from September to December around  $35^{\circ}$ ; it is latitudinally symmetric and out of phase with respect to the equator. This value is in agreement with the combination of DW2 (2K) and D0 (2K) from SABER at a similar altitude in September 2004. The oscillation is also noticed at  $35^{\circ}\text{N}$  in July and  $35^{\circ}\text{S}$  in March (4K).

395 The time series at 105 km is more structured. Maximum  $|n_{odd} - s|=1$  amplitudes occur ~~generally~~ mostly around  $30^\circ$  from  
November to March, particularly in the SH, and in July ~~(larger in the SH~~ (10K). The phase does not ~~significantly change~~  
~~along~~ change significantly over the year and is latitudinally asymmetric. This ~~contrasts the~~ is in contrast with behavior at lower  
altitudes, suggesting ~~main contribution of~~ other HME modes or ~~even tide components~~ even-parity frequency tidal components  
as principal contributions. The oscillation at 105 km is significant at the equator from October to December (6-8K) and is  
400 out-of-phase with that at  $30^\circ$ S.

These results are consistent with SABER measurements, showing D0 tide maxima at 110 km around  $30-40^\circ$ , particularly  
during the solstices and also strongest at SH local winter (7K), and DW2 maxima at 100-105 km over the equator, mainly from  
October to March (7K) (Gan et al., 2014; Truskowski et al., 2014). SABER also showed contribution from DW2 at  $35^\circ$ S but  
not in the NH, which could also be ~~the~~ responsible for the hemispheric asymmetry here.

405 Maxima at 105 km, out-of-phase with the ones at  $35^\circ$ S, appear around  $65^\circ$ N and S (6-8K) only during November-December.

### 3.3 The $|n_{odd} - s|=2$ mode

MIPAS  $|n_{odd} - s|=2$  longitudinal oscillation embeds the diurnal DE1 and DW3 and the terdiurnal TW1 ~~and TW2 components~~.  
~~The strongest signature among them is the DE1 components, of which DE1 is the strongest. These~~ non-migrating ~~tide and~~  
~~both are most likely originated by tides most likely arise from~~ non-linear interactions between their migrating ~~counterpart~~  
410 counterparts (DW1 and TW3, ~~respectively~~) ~~and the  $s = 1$  stationary planetary wave (SPW1).~~ and  $s = 2$  stationary planetary  
waves (SPW2).

~~Not many tidal analyses report on the~~ The detection of these ~~components~~ tidal components has been reported seldom in the  
past. Indeed, this mode is weaker than those with  $|n_{odd} - s|=0,1,4$  but it is a contribution with a coherent vertical propagation  
in MIPAS data above 90 km at certain latitudes (see below).

415 Figure 8 shows latitude-altitude maps of the derived amplitudes and phases for January and September. Both months show  
eastward propagating oscillations above 90 km at  $35^\circ$  South (2-5K) and North (3-8K in January and 3K in September).

September also exhibits a feature centered at  $5-10^\circ$ S above 75 km that mainly propagates ~~towards the west~~ westward and  
peaks at 90 km (6K). It is ~~not clear if unclear whether~~ the amplitudes measured around 110 km correspond uniquely to the  
same oscillation ~~alone~~ since there is no monotonical phase change with altitude. According to Truskowski et al. (2014), DW3  
420 vertical wavelength prevents its penetration into the thermosphere ~~, shall it be originated if it originates~~ in the troposphere.  
Therefore, the detection at these high altitudes ~~and the with~~ a lack of correspondence with an upward propagating signal could  
be consistent with a local source or with the propagation of a tidal ~~components~~ component different to DW3.

The wave spectrum derived from SABER in September around 110 km by Zhang et al. (2006) shows a contribution from  
DW3 at  $10-20^\circ$ S (6K) and  $40-50^\circ$ S (4K) and a small contribution from DE1 around  $20^\circ$ N ( $<4$ K). The direction of propa-  
425 gation of the waves derived here only coincide at  $35^\circ$ S. However, CMAM DE1 simulations of Ward et al. (2005) showed a  
symmetric three maxima latitudinal structure around 80-90 km dominating the mesopause (2K) and ~~turning to~~ converting into  
an asymmetric two maxima structure in the lower thermosphere. Thus, MIPAS  $|n_{odd} - s|=2$  structure probably responds to

the overlapping of two significant contributions, in which DW3 dominates at extra-tropical latitudes and DE1 dominates at the equator.

430 The time series of  $|n_{odd} - s|=2$  at 94 km shows a large seasonal variability. The maximum at 5-10°S appears mainly in May and September with a varying amplitude (bottom left panel in Fig. 8). The oscillation is also noticeable in March-April and September around 30-40°N and S, when the mode is latitudinally asymmetric. July and November reveal a 4K amplitude oscillation closer to the equator (20°) and latitudinally symmetric (in phase).

The time series at 105 km (bottom right panel of Fig. 8) shows an incoherent latitudinal pattern not clearly correlated to the  
435 one at 94 km. This suggests the contribution of high order Hough modes at higher altitudes, varying along throughout the year. ~~Strong signatures of~~ Whereas strong signatures for an anti-symmetric Hough mode are found for January (4-6K), April (2-4K) and July (2K), ~~whereas of~~ a symmetric mode in is indicated for September.

### 3.4 The $|n_{odd} - s|=3$ mode

The combination of the DE2 and the DW4 tides produces a  $|n_{odd} - s|=3$  longitudinal oscillation as seen by MIPAS. DE2  
440 ~~is originated by latent heat release~~ arises from the release of latent heat and its latitudinal/seasonal pattern is associated with a modulation by the mean wind (Pancheva et al., 2010). Fixed local time wavenumber-3 structures are present in the ionosphere but DE2 forcing from below has not yet been clearly determined (Pedatella et al., 2008; England et al., 2009; Pancheva and Mukhtarov, 2010)

~~The =3 mode~~ This is one of the dominating MIPAS zonal oscillations over the equator around 110 km in December  
445 (12K). Only the ~~=0 mode (migrating tides)~~ migrating component is stronger. ~~A latitudinally antisymmetric mode~~ It shows a latitudinally antisymmetric structure at 90 km ~~dominates MIPAS temperature amplitudes of =3~~ during December (see Fig. 9). The amplitudes maximize at tropical latitudes and are larger at 20°S (6K) than at 20°N (4K). ~~The phase dependence with altitude indicates contribution from an eastward propagating wave. The relative importance of the underlying Hough modes of this oscillation changes in the SH. A symmetric mode dominates above 100 km, where a symmetric mode dominates. In that~~  
450 ~~altitude region, amplitudes reach 15K and~~ amplitudes are significant at latitudes ~~smaller than below~~ 30-40°.

~~Amplitudes from 115-150 km during December also exhibit eastward propagation. Values amplify~~ Amplitudes increase up to 130-140 km (25K), where the oscillation starts ~~dissipation. This indicates~~ dissipating. This pattern of enhanced activity during the NH winter agrees with previous studies for DE2 (Pedatella et al., 2008) . MIPAS significant amplitudes in the E-region are not reproduced in the CTMT and the GSWM DE2, which model 5K maximum values above 110 km.

455 The phase increases with altitude (right upper plots of Fig. 9 and Fig. 10). If upward propagation is assumed, this indicates contribution from an eastward propagating wave. This indicates that, opposite to what Pancheva et al. (2010) state, DE2 may penetrate above 115 km but with a significantly longer vertical wavelength (30 km at 140 km in contrast ~~with to~~ 10-12 km in the upper mesosphere). ~~We note that this coherent latitude-altitude behavior at 115-150 km is not found for July. This may be caused by a weaker =3 oscillation then, which MIPAS does not clearly detect.~~

460 The change with altitude of the relative importance of the ~~Hough modes in =3 MIPAS mode happens~~ different Hough modes occurs throughout the year. This is deduced from the different latitudinal distribution of the amplitudes at 90 km and at 110 km

(bottom panels in Fig. 9). Amplitudes at 90 km ~~are maximum peak~~ during the solstices ~~at~~ around  $20^\circ$ . ~~They~~ (4-6K) and are larger in the local summer (5-6K) than in the local winter (3-4K). The oscillation also peaks in the solstices at 110 km (12K) and exhibits an off-equator displacement ( $5-10^\circ$ ) towards the local winter. ~~This result agrees~~ These results agree with the DE2 seasonal behavior derived from SABER (Pancheva et al., 2010; Pancheva and Mukhtarov, 2011). ~~MIPAS=3 phase around the equator at 110km moves  $20^\circ$  towards the west from December to July (not shown), also in agreement with SABER DE2.~~

### 3.5 The $|n_{odd} - s|=4$ mode

The  $|n_{odd} - s|=4$  MIPAS longitudinal variation includes the diurnal non-migrating components DE3 and DW5. These tidal modes are thought to be excited by diurnally-varying latent heat release over the wave-4 land-sea variation.  $|n_{odd} - s|=4$  also contains the TW1 and TW2 components. DE3 is the strongest non-migrating tidal effect in the lower thermosphere and has been widely studied. It is thought to be ~~the main responsible of~~ primarily responsible for the wave-4 structure detected at higher altitudes in the thermosphere (Hagan et al., 2007), while the direct absorption of the incoming radiation might play a secondary role (Achatz et al., 2008). It is not yet clear how much troposphere-originated DE3 contributes to the fixed local time zonal wavenumber-4 in the ionosphere (Oberheide et al., 2011a; Pedatella et al., 2012).

~~We note here that~~ MIPAS  $|n_{odd} - s|=4$  longitudinal oscillation has strong amplitudes in the lower thermosphere (at least below 135 km) over the equator.

Figure 11 shows ~~MIPAS=4~~ amplitudes and phases altitude-latitude cross-section derived for August. The amplitudes are significant from the equator to mid-latitudes above 70 km. They increase with altitude, reaching 8K around 95 km, 10K at 100 km, and ~~maximize at 125~~ peak at 120-125 km (35K). The mode starts ~~to dissipate~~ dissipating at 125 km but ~~keeps consistent~~ upward propagation (monotonically changing maintains a consistent vertical propagation (increasing phase with altitude)). The ~~peak at 125~~ DE3 temperature amplitude maximum is located around 110-115 km is 15 in results from CTMT and the Whole Atmosphere Model (WAM) (Akmaev et al., 2008) and about 5 km below in GSWM-09. MIPAS peak is around 10 km above the altitude predicted by models. This result may impact on the modeling of the mechanisms controlling DE3 maximum amplitude modeled by Oberheide and Forbes (2008a) for August.

~~MIPAS=4 generally weakens towards high latitudes. Its amplitude below 120~~ in the thermosphere. However, we note that the vertical resolution of MIPAS temperatures is approximately 10 km is smaller than 5K poleward to  $30^\circ$ . Nevertheless, our results reveal a local maximum in August at 120km (10K) and  $60^\circ$ . It is not clear if this peak is related to the signals measured at these latitudes at lower altitudes (2K at 90-100km and 2-4K-110km). these altitudes, enough to shift the peak and partially explain the difference.

The  $|n_{odd} - s|=4$  phase ~~moves westward as latitude increases~~ decreases with latitude, so that the oscillations over the equator and at  $20-25^\circ$  are out of phase. ~~The phase moves eastward as altitude increases~~ The phase increases with altitude, pointing to DE3 as the main contributor if an upward propagation is assumed. The vertical wavelength in the mesosphere is 8-12 km. The phase plot exhibits a crosswise structure, which ~~softens~~ decreases with height until the lower thermosphere, where the phase is almost latitudinally symmetric. This indicates the presence of an asymmetric HME mode below 95 km, that is more

495 efficiently dissipated as it propagates upwards than the symmetric ones. This confirms the results for the DE3 HMEs of [the CTMT](#) Oberheide and Forbes (2008a). In the lower thermosphere, the vertical wavelength increases to 20 km.

Latitude-time slices at ~~84, 94, 110 and 125 km selected altitudes~~ are plotted in Fig. 12. Maximum amplitudes ~~at 84 km~~ occur around 10-20°. ~~They show up only in the SH in January and July and N and 10-20°S at 84 km, stronger in the NH in April and September-October. There are North and South pairs the rest of the year but the NH oscillation is always stronger (7K vs. 4K). Thus, the oscillation.~~ [There oscillation](#) tilts to the North during the equinoxes, to the South at the beginning of the NH Winter, and is latitudinally extended and centered over the equator, ~~as a Kelvin wave,~~ during the NH summer, [agreeing with the DE3 pattern from SABER \(Gan et al., 2014; Zhang et al., 2006\) and MLS \(Forbes and Wu, 2006\)](#). The 4K larger MIPAS amplitudes might be explained by contribution from DW5. Non-negligible amplitudes ~~appear also~~ [also appear in MIPAS data](#) at high latitudes, at 60° in July and at 80-85° in November.

505 ~~The latitudinal tilt at low latitudes at 84 km agrees with findings for DE3 from SABER (Gan et al., 2014; Zhang et al., 2006) and MLS (Forbes and Wu, 2006) for particular seasons. The 4K larger MIPAS =4 amplitudes are most probably due to the added contribution from DW5. Zhang et al. (2006) estimated DW5 amplitudes of 2K in September 2004 SABER.~~

~~MIPAS =4 oscillation~~ [Large amplitudes mainly occur around the equator](#) at 94 km ~~shows large amplitudes mainly around the equator (5-8K), consistent with SABER DE3 (Gan et al., 2014) but 2K larger. Values maximize, maximizing (6-8K)~~ from June to September ~~and minimize in January. The phase slightly changes through the year, although generally occurs over Greenwich. The seasonal behavior (Fig. 12), 2K larger than SABER DE3 (see e.g. Gan et al., 2014). This seasonal pattern agrees with a cycle responding to the combined seasonal variation of the background atmosphere and of the diurnal heat source (Oberheide et al., 2006; Achatz et al., 2008). Exceptions to this general behavior occur in MIPAS data in November-December, showing peaks at 15°N and S (MIPAS also measures 5K), and in February, with peaks at 20°N (5K). Expansion of the mode to higher latitudes (maxima close to the tropics in November-December and February and high latitude (50-60°) also occurs activity~~ in July-August ~~at this altitude.~~

The oscillation is significantly amplified at 110 km ([10-15K](#)) and 125 km (~~Fig. 12~~). ~~The seasonal variability equatorward of 20-30° is similar (30K) but has a similar seasonal variability~~ to that at lower altitudes. ~~Significant amplitudes are measured from July to October and from March to May (10-15K at 110 km and 30K at 125 km).~~ MIPAS values at 110 km ~~agree in general~~ [generally agree](#) with those derived from SABER for DE3 at similar altitudes (Zhang et al., 2006; Gan et al., 2014), although they are larger (2K) in March. DW5 contribution is also expected at these altitudes (a maximum of 4K, according to SABER).

This mode also ~~present~~ [presents](#) hemispherically symmetric signatures at 50-60° in July-August at 110 km (2-4K) and 125 km (10K) and in November at 80° at 110 km (4K).

525 The phase at 110 km varies [throughout the year](#) over the equator ~~along the year~~ (not shown). It shifts towards the West ~~as latitude increases with latitude~~ or, in terms of local time phase and assuming a dominant eastward propagating component (DE3), it occurs ~~later~~ [later](#) in the day. The phase generally presents hemispherical symmetry.

The seasonal behavior reflects ~~, in general at all altitudes,~~ the seasonal change of the relative importance of the different Hough modes [for most altitudes](#). There is a ~~major~~ [major](#) contribution from a symmetric mode ~~all over~~ [throughout](#) the year at

530 thermospheric altitudes, except from November to January. ~~Then, it is~~ It is then overcome (95-110 km) or competes (around 125 km) with an anti-symmetric mode, in agreement with HME from Oberheide and Forbes (2008a). July also presents a small contribution from the symmetric mode around 125 km. However, it is then when the asymmetric mode is strongest, whereas Oberheide and Forbes (2008a) report it to be strongest only in January.

#### 4 Inter-annual variability

535 Five years of continuous observations are ~~not enough~~ insufficient to unambiguously link atmospheric processes through correlations but ~~enough are adequate~~ to check for tidal quasi-biennial oscillations (QBO). Year to year variability of strengths of the measured longitudinal oscillations due to the effect of the ~~effect from the~~ zonal wind Quasi-Biennial-Oscillation is expected ~~(McLandress, 2002; Mayr and Mengel, 2005)~~ (McLandress, 2002; Mayr and Mengel, 2005; Huang et al., 2006; Xu et al., 2009). Oberheide et al. (2009) and references therein discuss ~~on~~ the possible mechanisms through which the zonal wind QBO might  
540 affect daily temperature oscillations.

At each altitude and latitude, we have decomposed the amplitudes of MIPAS  $\Delta T/2$  derived  $|n_{odd} - s|$  longitudinal oscillation modes from 2007 to 2012 ~~in into~~ six intra-annual sinusoidal components (with 12, 6, 4, 3, 2.4 and 2 month periods), an inter-annual sinusoidal component (with its period as a free parameter) and a component proportional to the solar flux. We have allowed for solar cycle effects, for which we ~~accurately know~~ have accurate input energy variation, with the ~~only sole~~ aim of  
545 deriving a more accurate inter-annual oscillation. Note that MIPAS time coverage spans from solar minimum to solar maximum and, thus, all monotonical variations of temperature amplitudes, like trends, are embedded in this solar component. We have unambiguously found inter-annual variations consistent with a QBO in MIPAS data only for the strong  $|n_{odd} - s|=0$  mode. ~~The A QBO in the DE3 component should also present a QBO (Li et al., 2015) but small and it is not surprising that we could no detect it is not detected~~ in MIPAS data. This is not surprising as the impact of the QBO on DE3 is expected to be small  
550 (Li et al., 2015).

Figure 13 shows ~~typical time series for which we perform the decomposition at each altitude. The examples shown are for MIPAS derived the time series from 2007 to 2012 of MIPAS  $|n_{odd} - s|=0$  amplitudes from monthly zonal means from 2007 to 2012 over the equator and at 35°N. In the case of the analysis of the variations of the  $=0$  oscillations with time at a given altitude, we recall that MIPAS  $=0$  values correspond to the amplitudes of a tidal component~~ We recall that these correspond  
555 to migrating tide total amplitudes only at the altitudes ~~for which its where the tidal~~ phase or anti-phase is 10Å.M., which ~~corresponds to are approximately located at~~ the peaks in the vertical profiles. We already mentioned in ~~Seet~~ Section 3.1 that there is a seasonal variation in the altitudes of these peaks, particularly ~~at~~ at extra-tropical latitudes. ~~The altitudes of the  $=0$  maxima vary along~~ These altitudes vary during a calendar year ~~as much as~~ 2 km up and down around 78 km and 85 km over the equator, but as much as 5 km around 75 km and 3 km at 88 km at 35°N, being higher in the winter (Fig. 13). This also  
560 happens in the Southern hemisphere SH but to a ~~significant~~ significantly lesser extent (not shown). ~~This change~~ These changes of peak altitudes ~~represents are most likely due to a change of phase but not of vertical wavelength because the~~. The vertical wavelength barely changes because the peak altitude shift occurs at most altitudes simultaneously.

This behavior is repeated ~~every year~~annually, pointing to a persistent seasonal effect.

~~The varying peak altitudes could be originated by~~ It could arise from a seasonal change of the relative contribution from the  
565 different sources of this component, namely, the semi-annually varying background atmosphere and symmetry of the heating  
source. Due ~~of to~~ its hemispherical asymmetry, we attribute it to the annual oscillation of the background atmosphere, signifi-  
cantly larger in the NH. Interaction with other dynamical features during the winter are not ruled out. ~~This behavior also shows~~  
~~that one should be cautious when interpreting zonal mean intra-annual variability at fixed altitudes from a sun-synchronous~~  
~~instrument data, like MIPAS, because one could be sounding changes of phase of tidal components. Nevertheless, as the change~~  
570 ~~of the altitude of the peaks at a given month from year to year is not significant, the inter-annual variability can be safely~~  
~~extracted.~~

A QBO in ~~the MIPAS~~  $|n_{odd} - s|=0$  mode amplitudes is noticeable in Fig. 13, particularly at ~~low latitudes and even in~~  
~~the middle atmosphere~~the equator. Figure 14 shows ~~MIPAS =0 amplitudes from 2007 to 2012~~ these time series at 44, 76  
and 86 km over the equator (approximate peaking altitudes in the equinoxes) and the fitted annual, semi-annual and inter-  
575 annual components. Note that we kept the sign of the perturbations. The inter-annual component (red) competes with the  
combination of the semi-annual ~~oscillation (light blue)~~ and the annual oscillations (grey) below 80 km. We also show two dif-  
ferent representations of the zonal wind stratospheric QBO (SQBO) in Fig. 14: that obtained at the NOAA-ESRL Physical  
Sciences Division from the zonal average of the 30 mb zonal wind at the equator calculated from the NCEP/NCAR Re-  
analysis (<http://www.esrl.noaa.gov/psd/>) and that measured at 30 mb from a radiosonde station in Singapore, compiled by the  
580 Freie Universitaet Berlin (<http://www.geo.fu-berlin.de/en/met/ag/strat/produkte/qbo/index.html>). The ~~period of the inter-annual~~  
~~component (red) of =0 agrees with that of the Singapore winds.~~

~~Ekanayake et al. (1997) found that longitudinally propagating tides are generally larger for mean zonal winds blowing in the~~  
~~opposite direction. That implies that DW1 (or TW3), a westward propagating tide, should be larger for westerlies. The~~ phase  
of the background zonal wind SQBO at 30 mb is opposite to that of the mesospheric QBO (MQBO) (Burrage et al., 1996)-  
585 ~~Therefore, the effect of SQBO on a tide should be opposite to that of the MQBO,~~ that is, when the SQBO is in its westerly  
phase, the MQBO is in its easterly phase.

The period of the derived inter-annual component (red) of MIPAS  $|n_{odd} - s|=0$  ~~strengthens~~ agrees with that of the Singapore  
winds at all altitudes ~~simultaneously during the zonal wind SQBO westerly phase~~ (see Fig. 14), ~~that is, the~~. The (absolute  
value) of this inter-annual component is in phase with the zonal wind SQBO. In other words, MIPAS  $|n_{odd} - s|=0$  strengthens at  
590 all altitudes simultaneously during the SQBO westerly phase, in agreement with previous observational studies (Xu et al., 2009; Wu et al., 2009)  
and, therefore, the MQBO easterly phase. ~~That suggest then that the effect on tides is produced~~ Ekanayake et al. (1997) found  
that longitudinally propagating tides are stronger for mean zonal winds blowing in the opposite direction, which implies that  
a westward propagating tide, like DW1, should be stronger for westerlies. In combination, these facts suggest that the QBO  
effect on mesospheric migrating tides is mainly not produced locally by the zonal wind SQBO, although an additional local  
595 ~~smaller effect in the mesosphere by the MQBO could also be possible~~ MQBO. A more likely possibility is a zonal wind QBO  
interaction with tides in the stratosphere. This supports the argument by (Forbes and Vincent, 1989) of varying stratospheric  
tide filtering during upward propagation caused by the varying mean zonal winds instead of a ~~more plausible~~ local effect in the

mesosphere, where dissipation starts (~~Oberheide et al., 2009~~), as Oberheide et al. (2009) suggested as more plausible for DE3. Note that inter-annual variation at tropospheric altitudes, where the tide mainly originates, can not be ruled out.

600 A QBO ~~also appears~~ is also present everywhere else where MIPAS  $|n_{odd} - s| = 0$  mode is significant: there are stronger migrating tides during the SQBO eastward phase. Figure 15 shows ~~its QBO-derived amplitude. Once more, we recall that MIPAS measures the total QBO effect only at the altitudes where  $=0$  amplitudes are maximum. The QBO oscillation of the  $=0$  mode has amplitudes~~ a map of the QBO amplitude. Values are smaller than 0.5K ~~amplitudes~~ below 75 km over the equator and below 105 km around 30° ~~North and South~~ N and 30°S, 1K at 76 km, 2K at 86 km, 1K at 98 km and 1.5K at 110 km. These  
605 results agree with those derived from SABER below 90 km (Xu et al., 2009). Above, SABER values are about 1K larger.

## 5 Summary

The sun-synchronous Michelson Interferometer for Passive Atmospheric Sounding (MIPAS) globally sounded the atmospheric limb from the stratosphere to the lower thermosphere ~~in a global scale~~. MIPAS took measurements at two fixed local times during its ~~descending~~ ascending (10 A.M.) and descending (10 P.M.) nodes. Subtraction of the descending and ascending node  
610 measurement pairs,  $\Delta T/2$ , at each latitude, altitude and longitude eliminate the background atmosphere, the ~~persistent (on a daily basis)~~ daily-invariant longitudinal oscillations (like planetary waves) and also the longitudinal oscillations with daily frequencies such that they are an even integer factor of the 24-hour day (like semi-diurnal tides). Thus, the zonal variation of the  $\Delta T/2$  depicts a 'solar-view' mainly of the diurnal and terdiurnal tidal components.

Extraction of the underlying longitudinal oscillations by spectral analysis isolates the amplitudes and phases of the contributing  
615 MIPAS zonal wavenumbers  $k$  contributing. Each wavenumber  $k$  comprises the combined contribution of the tidal modes fulfilling such that their daily frequency  $n$ , an odd integer, and their zonal wavenumber  $s$ , are  $|n_{odd} - s| = k$ . The tidal modes embedded in MIPAS  $k$  modes are listed in Table 1.

MIPAS spectra covered the CO<sub>2</sub> 15  $\mu\text{m}$  and NO 5.3  $\mu\text{m}$  emissions from which temperatures from ~~20-40~~ to 150 km are derived. We ~~have~~ extracted the wavenumber  $k = 0 - 4$  longitudinal waves from these temperatures globally from April 2007  
620 to March 2012 ~~in a global scale and make and have made~~ them available to the scientific community. To our knowledge, this is the first time ~~temperature zonal oscillations~~ zonal oscillations in temperature are derived in this altitude range globally from a single instrument.

We analyze and characterize the behavior of MIPAS  $|n_{odd} - s|$  ~~temperature~~ longitudinal oscillations from a climatological point of view from averages of monthly mean MIPAS  $\Delta T/2$ . ~~The results agree well in general~~ The results generally agree well  
625 with measurements from other instruments, like SABER or MLS. They reveal that:

- Migrating tidal perturbations with odd  $n$  below 105 km are ~~as expected~~, stronger during the equinoxes. They are latitudinally symmetric in strength. Their phases exhibit a seasonal variation, with a delay in the winter months that is larger in the Northern hemisphere. The dominating tidal mode at latitudes ~~smaller than~~ below 50°, probably the first mode of the upward propagated DW1, rapidly dissipates above 105 km.

- 630 – At 110 km, the ~~major migrating contribution is most likely TW3. Maxima are generally reached at combination of the~~  
diurnal and terdiurnal migrating tide contributions produces maxima around 35° ,with a N and 35°S from September  
to May and from 35°N to 35°S from June to August. They shift 5° shift to higher latitudes in the local summer. TW3  
might also be responsible ~~of for~~ the strong migrating perturbations measured at 120 km ~~.Another possibilities are but~~  
635 contributions from an upward propagated DW1 high order mode or from the *in situ* generated thermospheric tide are  
also a possibility.
- The thermospheric DW1 above 130 km produces maximum perturbations off the equator, tracking the sub-solar point  
and ~~maximizing peaking~~ in the local summer.
- MIPAS measured impact from migrating tides with  $n - odd$  at Southern high latitude summer, with alternating maxima  
and minima at 90 and 100 km in phase with those at 35°. This agrees with previous ~~ground based ground based~~  
640 (Lübken et al., 2011). MIPAS additionally detected a weaker counterpart in the NH summer.
- Besides equatorial,  $|n_{odd} - s|=1$  also exhibits extra-tropical (35°) and high-latitude (65°) activity in the MLT, particularly  
in the SH from November to January.
- $|n_{odd} - s|=2$  presents significant seasonal variability with a latitudinal structure responding to ~~overlapping the overlap~~  
of two contributions, a westward propagating oscillation that dominates at extra-tropical latitudes and an eastward prop-  
645 agating one that dominates at the equator.
- $|n_{odd} - s|=3$  is the strongest non-migrating mode in December ~~.An eastward propagating wave ,and is also noticeable~~  
in November and January. A wave tilting eastward with altitude and already detected at 70 km, penetrates well in the  
lower thermosphere with a significantly larger vertical wavelength than in the mesosphere.
- MIPAS shows a prominent wavenumber 4 structure starting at 70 km and ~~maximizing peaking~~ around 135 km (15 km  
650 above results from models). The latitudinal distribution reveals a contribution from a symmetric Hough mode in the  
lower thermosphere, which propagates upwards more easily than the antisymmetric one dominating in the mesosphere.
- $|n_{odd} - s|=4$  expands to higher latitudes in July-August, when hemispherically symmetric footprints are detected at  
50-60° above 85 km. Signatures of this mode are also detected in November at 80°.

We ~~have~~ also studied the inter-annual variability of the amplitudes of the MIPAS  $|n_{odd} - s|$  wavenumbers derived from  
655 monthly mean MIPAS  $\Delta T/2$ . We unambiguously detect a  $|n_{odd} - s|=0$  ~~Quasi-Biennial Oscillation~~ QBO, reaching 2K in the  
upper mesosphere at low latitudes. Comparison of tidal ~~QBO~~ and zonal wind stratospheric and mesospheric QBO phases  
suggests that the QBO effect on tides ~~occurs mainly in the stratosphere and is afterwards propagated upwards~~ does not mainly  
occur in the mesosphere.

The good MIPAS temporal resolution and global coverage observations extending from the stratosphere to the lower thermo-  
660 sphere presented here are useful for testing general circulation models considering tidal effects in the MLT region and may well

represent a challenge for them to model their vertical, latitudinal and temporal dependence. A thorough analysis of particular cases found here is needed and will be [the](#) focus of future work.

## Appendix A: Methodology for extraction of odd parity daily frequency tidal components

665 Considering the effect of tides as the only source of longitudinal variability, an atmospheric variable  $X$  (like temperature or species concentration) measured at longitude  $\lambda$ , altitude  $z$ , latitude  $\phi$  and local solar time  $t$  can be described as the variable zonal mean  $\bar{X}$  at  $z$  and  $\phi$  perturbed by the sum of the tidal oscillations  $X'_{n,s}$ , with zonal wavenumber  $s$  and daily wave frequency  $n$ , at position  $(\lambda, z, \phi)$  and time  $t$ :

$$X(\lambda, t) = \bar{X} + \sum_{n,s} X'_{n,s}(\lambda, t), \quad (\text{A1})$$

670 where, for clarity, the dependence of  $X$ ,  $\bar{X}$  and  $X'_{n,s}$  on  $z$  and  $\phi$  is not written. The tidal oscillations can be expressed as sinusoidal longitudinal oscillations of the form (e.g. Williams and Avery, 1996):

$$X'_{n,s}(\lambda, t) = A_{n,s} \cos(n\Omega t - (n-s)\lambda + \Phi_{n,s}). \quad (\text{A2})$$

675 where  $\Omega = 2\pi/24$  is the Earth's angular velocity, and the oscillation amplitude  $A_{n,s}$  and phase  $\Phi_{n,s}$  are functions of  $z$  and  $\phi$ . Note that this expression can be easily expressed in terms of Universal Time  $t'$  using  $t = t' + \frac{24}{2\pi}\lambda$ . The zonal wavenumber  $s \in \mathbb{Z}$  is defined such that  $s < 0$  refers to eastward propagating tides,  $s > 0$  to westward propagating tides and  $s = 0$  to stationary tides. The daily wave frequency  $n \in \mathbb{N}$  is a positive integer such that  $n = 1$  for a diurnal component,  $n = 2$  for a semi-diurnal component, and so on.

For the particular case of sun-synchronous instrument observations, the local solar time of the ascending and descending segments,  $t_a$  and  $t_d$ , are fixed and fulfill  $t_a = t_d + 12$ . A tidal perturbation at local time  $t_a$ ,  $X'_{n,s}(\lambda, t_a)$ , is then related to that at  $t_d$ ,  $X'_{n,s}(\lambda, t_d)$ , through:

$$\begin{aligned} X'_{n,s}(\lambda, t_a) &= A_{n,s} \cos(n\Omega t_a - (n-s)\lambda + \Phi_{n,s}) = \\ &= A_{n,s} \cos(n\Omega t_d + n\pi - (n-s)\lambda + \Phi_{n,s}) = \\ 680 \quad &= (-1)^n X'_{n,s}(\lambda, t_d). \end{aligned} \quad (\text{A3})$$

Therefore, half the difference of the variable observed at longitude  $\lambda$  at the descending node local time  $X(\lambda, t_d)$  and at the ascending node local time  $X(\lambda, t_a)$  is:

$$\Delta X/2 = \frac{X(\lambda, t_d) - X(\lambda, t_a)}{2} = \frac{1}{2} \left[ \sum_{n,s} X'_{n,s}(\lambda, t_d) - \sum_{n,s} (-1)^n X'_{n,s}(\lambda, t_d) \right] = \sum_{n-\text{odd}} \sum_s X'_{n,s}(\lambda, t_d), \quad (\text{A4})$$

where addends with even  $n$  and  $n = 0$  (stationary longitudinal oscillations) cancel out.

685 Defining  $k = |n - s|$ , with  $k \in \mathbb{N}$ ,  $\Delta X/2$  in Eq. A4 can be written as:

$$\Delta X/2 = \sum_{n-\text{odd}} X'_{n,n}(t_d) + \sum_{n-\text{odd}, s < n} X'_{n,s}(\lambda, t_d) + \sum_{n-\text{odd}, s > n} X'_{n,s}(\lambda, t_d) = \sum_{n-\text{odd}} X'_{n,n}(t_d) + \sum_k \sum_{n-\text{odd}} X'_{n,n-k}(\lambda, t_d) + X'_{n,n+k}(\lambda, t_d).$$

Since  $t_d$  is fixed,  $\Delta X/2$  is a function of longitude that can be Fourier-decomposed at each  $z$  and  $\phi$ ,  $\Delta X/2 = C_0 + \sum_k C_k \cos(k(\lambda - \theta_k))$ . Making a term-to-term correspondence of this harmonic decomposition with the right hand side of Eq. A5 and using Eq. A2, each  $k$ -order Fourier term equals to:

$$\begin{aligned}
 C_k \cos(k(\lambda - \theta_k)) &= \sum_{n\text{-odd}} X'_{n,n-k}(\lambda, t_d) + X'_{n,n+k}(\lambda, t_d) = \\
 690 \quad &= \sum_{n\text{-odd}} A_{n,n\pm k} \cos(n\Omega t_d \pm k\lambda + \Phi_{n,n\pm k}). \tag{A6}
 \end{aligned}$$

$k$ 's are *apparent* longitudinal wavenumbers of the  $\Delta X/2$  decomposition. Modes fulfilling that  $n$  is odd and  $s = n \pm k$  appear to have a  $k$  wavenumber on the sun-synchronous instrument  $\Delta X/2$  and, thus, combine and are embedded in the the  $k = |n - s|$  term. We hereafter denote this combined oscillation as  $|n_{\text{odd}} - s| = k$ . The major tidal components contributing to each apparent zonal wavenumber  $k$  are listed in Table 1.

705 Even if the tidal modes with the same  $n$  parity and the same  $|n - s|$  are aliased, a close look at the derived phases  $\theta_k$  and their dependence with altitude ultimately helps discern the dominance of a certain direction of horizontal propagation.

The zero order Fourier term equals to:

$$C_0 = \sum_{n\text{-odd}} X'_{n,n}(t_d) = \sum_{n\text{-odd}} A_n \cos(n\Omega t_d + \Phi_{n,n}), \tag{A7}$$

700 that is, the addition of the solar migrating components ( $s = n$ ), which do not depend on  $\lambda$  but only on local time  $t_d$ . This equation shows that, even if only one mode dominates, the derived amplitude  $C_0$  only corresponds to the amplitude of the tidal component  $A_{n,n}$  at the altitudes where the phase  $\Phi_{n,n}$  is  $n\Omega t_d$  or  $n\Omega t_d + \pi$ . These altitudes show up as maxima (or minima) in the derived  $C_0$  vertical profile. Another piece of information comes from the vertical nodes of that profile, corresponding to altitudes for which the phase is  $n\Omega(t_d \pm \pi/2)$ .

705 A method similar to the one described here was successfully applied to CRISTA data initially by Oberheide et al. (2002) and recently to SABER and MLS data by Lieberman et al. (2015). Li et al. (2015) also present an analogous analysis but applied to any two fixed local times for the descending and the ascending nodes. In the later case, the isolation of individual tidal components is then possible if only two daily frequencies  $n$  contribute.

Analogously to the subtraction, the sum of the variable pairs measured at the descending and at the ascending node LSTs at longitude  $\lambda$  allows for the determination of the  $n - \text{even}$  modes.

710 *Acknowledgements.* MGC was financially supported by the MINECO under its 'Ramon y Cajal' subprogram. The IAA team was supported by the Spanish MINECO, under project ESP2014-54362-P, and EC FEDER funds. IMK/IAA generated MIPAS data can be accessed [after by request at https://www.imk-asf.kit.edu/english/1500.php](https://www.imk-asf.kit.edu/english/1500.php).

## References

- Achatz, U., Grieger, N., and Schmidt, H.: Mechanisms controlling the diurnal solar tide: Analysis using a GCM and a linear model, *J. Geophys. Res.*, 113, A08303, doi:10.1029/2007JA012967, 2008.
- 715 Akmaev, R. A., Fuller-Rowell, T. J., Wu, F., Forbes, J. M., Zhang, X., Anghel, A. F., Iredell, M. D., Moorthi, S., and Juang, H.-M.: Tidal variability in the lower thermosphere: Comparison of Whole Atmosphere Model (WAM) simulations with observations from TIMED, *Geophys. Res. Lett.*, 35, L03 810, doi:10.1029/2007GL032584, 2008.
- Beig, G., Keckhut, P., Lowe, R. P., Roble, R. G., Mlynczak, M. G., Scheer, J., Fomichev, V. I., Offermann, D., French, W. J. R., Shepherd, M. G., Semenov, A. I., Remsberg, E. E., She, C. Y., Lübken, F. J., Bremer, J., Clemesha, B. R., Stegman, J., Sigernes, F., and Fadnavis, S.: Review of mesospheric temperature trends, *Rev. Geophys.*, 41, doi:10.1029/2002RG000121, 2003.
- 720 Bermejo-Pantaleón, D., Funke, B., López-Puertas, M., García-Comas, M., Stiller, G. P., von Clarmann, T., Linden, A., Grabowski, U., Höpfner, M., Kiefer, M., Glatthor, N., Kellmann, S., and Lu, G.: Global Observations of Thermospheric Temperature and Nitric Oxide from MIPAS spectra at 5.3  $\mu\text{m}$ , *J. Geophys. Res.*, 116, A10313, doi:10.1029/2011JA016752, <http://dx.doi.org/10.1029/2011JA016752>, 2011.
- 725 Bruinsma, S. L. and Forbes, J. M.: Anomalous behavior of the thermosphere during solar minimum observed by CHAMP and GRACE, *Journal of Geophysical Research (Space Physics)*, 115, A11323, doi:10.1029/2010JA015605, 2010.
- Burrage, M. D., Vincent, R. A., Mayr, H. G., Skinner, W. R., Arnold, N. F., and Hays, P. B.: Long-term variability in the equatorial middle atmosphere zonal wind, *J. Geophys. Res.*, 101, 12 847, doi:10.1029/96JD00575, 1996.
- 730 Chapman, S. and Lindzen, R. S.: *Atmospheric Tides*, Reidel, Dordrecht, Netherlands, 1970.
- Cho, Y.-M. and Shepherd, G.: Resolving daily wave 4 nonmigrating tidal winds at equatorial and midlatitudes with WINDII: DE3 and SE2, *Journal of Geophysical Research (Space Physics)*, 120, 10, doi:10.1002/2015JA021903, 2015.
- Chu, Y.-H., Wu, K.-H., and Su, C.-L.: A new aspect of ionospheric E region electron density morphology, *Journal of Geophysical Research (Space Physics)*, 114, A12 314, doi:10.1029/2008JA014022, 2009.
- 735 Davis, R. N., Du, J., Smith, A. K., Ward, W. E., and Mitchell, N. J.: The diurnal and semidiurnal tides over Ascension Island ( $^{\circ}$  S,  $14^{\circ}$  W) and their interaction with the stratospheric quasi-biennial oscillation: studies with meteor radar, eCMAM and WACCM, *Atmospheric Chemistry & Physics*, 13, 9543–9564, doi:10.5194/acp-13-9543-2013, 2013.
- Du, J. and Ward, W. E.: Terdiurnal tide in the extended Canadian Middle Atmospheric Model (CMAM), *Journal of Geophysical Research (Atmospheres)*, 115, D24106, doi:10.1029/2010JD014479, 2010.
- 740 Eckermann, S. D. and Marks, C. J.: An idealized ray model of gravity wave-tidal interactions, *J. Geophys. Res.*, 101, 21 195, doi:10.1029/96JD01660, 1996.
- Ekanayake, E. M. P., Aso, T., and Miyahara, S.: Background wind effect on propagation of nonmigrating diurnal tides in the middle atmosphere, *J. Atmos. Sol.-Terr. Phys.*, 59, 401–429, doi:10.1016/S1364-6826(96)00012-0, 1997.
- England, S. L., Maus, S., Immel, T. J., and Mende, S. B.: Longitudinal variation of the E-region electric fields caused by atmospheric tides, *Geophys. Res. Lett.*, 33, L21 105, doi:10.1029/2006GL027465, 2006.
- 745 England, S. L., Zhang, X., Immel, T. J., Forbes, J. M., and DeMajistre, R.: The effect of non-migrating tides on the morphology of the equatorial ionospheric anomaly: seasonal variability, *Earth, Planets, and Space*, 61, 493–503, doi:10.1186/BF03353166, 2009.
- Fischer, H., Birk, M., Blom, C., Carli, B., Carlotti, M., von Clarmann, T., Delbouille, L., Dudhia, A., Ehhalt, D., Endemann, M., Flaud, J. M., Gessner, R., Kleinert, A., Koopmann, R., Langen, J., López-Puertas, M., Mosner, P., Nett, H., Oelhaf, H., Perron, G., Remedios, J.,

- 750 Ridolfi, M., Stiller, G., and Zander, R.: MIPAS: an instrument for atmospheric and climate research, *Atmos. Chem. Phys.*, 8, 2151–2188, 2008.
- Forbes, J. M. and Garrett, H. B.: Solar diurnal tide in the thermosphere, *J. Atmos. Sci.*, 33, 2226–2241, doi:10.1175/1520-0469(1976)033<2226:SDTITT>2.0.CO;2, 1976.
- Forbes, J. M. and Garrett, H. B.: Theoretical studies of atmospheric tides, *Reviews of Geophysics and Space Physics*, 17, 1951–1981, 755 doi:10.1029/RG017i008p01951, 1979.
- Forbes, J. M. and Hagan, M. E.: Thermospheric extensions of the classical expansion functions for semidiurnal tides, *J. Geophys. Res.*, 87, 5253–5259, doi:10.1029/JA087iA07p05253, 1982.
- Forbes, J. M. and Vincent, R. A.: Effects of mean winds and dissipation on the diurnal propagating tide - An analytic approach, *Planet. Spa. Sci.*, 37, 197–209, doi:10.1016/0032-0633(89)90007-X, 1989.
- 760 Forbes, J. M. and Wu, D.: Solar tides as revealed by measurements of mesosphere temperature by the MLS experiment on UARS, *J. Atmos. Sci.*, 63, 1776–1797, 2006.
- Forbes, J. M., Zhang, X., and Hagan, M. E.: Simulations of diurnal tides due to tropospheric heating from the NCEP/NCAR Reanalysis Project, *Geophys. Res. Lett.*, 28, 3851–3854, doi:10.1029/2001GL013500, 2001.
- Forbes, J. M., Zhang, X., Palo, S., Russell, J., Mertens, C. J., and Mlynczak, M.: Tidal variability in the ionospheric dynamo region, *Journal of Geophysical Research*, 113, A02 310, 2008. 765
- Forbes, J. M., Bruinsma, S. L., Zhang, X., and Oberheide, J.: Surface-exosphere coupling due to thermal tides, *Geophys. Res. Lett.*, 36, L15 812, doi:10.1029/2009GL038748, 2009.
- Forbes, J. M., Zhang, X., and Bruinsma, S. L.: New perspectives on thermosphere tides: 2. Penetration to the upper thermosphere, *Earth, Planets, and Space*, 66, 122, 2014.
- 770 Fritts, D. C. and Vincent, R. A.: Mesospheric momentum flux studies at Adelaide, Australia - Observations and a gravity wave-tidal interaction model, *Journal of Atmospheric Sciences*, 44, 605–619, doi:10.1175/1520-0469(1987)044<0605:MMFSAA>2.0.CO;2, 1987.
- Funke, B., López-Puertas, M., García-Comas, M., Kaufmann, M., Höpfner, M., and Stiller, G. P.: GRANADA: a Generic RADIative traNsfer AnD non-LTE population Algorithm, *J. Quant. Spectrosc. Radiat. Transfer*, 113, 1771–1817, doi:10.1016/j.jqsrt.2012.05.001, http://dx.doi.org/10.1016/j.jqsrt.2012.05.001, 2012.
- 775 Gan, Q., Du, J., Ward, W. E., Beagley, S. R., Fomichev, V. I., and Zhang, S.: Climatology of the diurnal tides from eCMAM30 (1979 to 2010) and its comparison with SABER, *Earth, Planets, and Space*, 66, 103, doi:10.1186/1880-5981-66-103, 2014.
- García-Comas, M., Funke, B., López-Puertas, M., Bermejo-Pantaleón, D., Glatthor, N., Clarmann, T. v., Stiller, G. P., Grabowski, U., Boone, C. D., French, W. J., Leblanc, T., López-González, M. J., and Schwartz, M.: On the Quality of MIPAS Kinetic Temperature in the Middle Atmosphere, *Atmos. Chem. Phys.*, 12, 6009–6039, doi:10.5194/acp-12-6009-2012, http://www.atmos-chem-phys.net/12/6009/2012/, 780 2012.
- García-Comas, M., Funke, B., Gardini, A., López-Puertas, M., Jurado-Navarro, A., von Clarmann, T., Stiller, G., Kiefer, M., Boone, C. D., Leblanc, T., Marshall, B. T., Schwartz, M. J., and Sheese, P. E.: MIPAS temperature from the stratosphere to the lower thermosphere: Comparison of vM21 with ACE-FTS, MLS, OSIRIS, SABER, SOFIE and lidar measurements, *Atmos. Meas. Tech.*, 7, 3633–3651, doi:10.5194/amt-7-3633-2014, http://www.atmos-meas-tech.net/7/3633/2014/, 2014.
- 785 García-Comas, M., et al., and et al.: MIPAS observations of longitudinal oscillations in the mesosphere and the lower thermosphere: Part 2. Climatology of even-parity daily frequency modes, *Atmos. Chem. Phys.*, doi:in preparation, 2015.

- Gurubaran, S., Rajaram, R., Nakamura, T., and Tsuda, T.: Interannual variability of diurnal tide in the tropical mesopause region: A signature of the El Nino-Southern Oscillation (ENSO), *Geophysical Research Letters*, 32, 13 805, doi:10.1029/2005GL022928, 2005.
- 790 Hagan, M. and Forbes, J.: Migrating and nonmigrating diurnal tides in the middle and upper atmosphere excited by tropospheric latent heat release, *J. Geophys. Res.*, 107, 4754, <http://dx.doi.org/10.1029/2001JD001236>, 2002.
- Hagan, M. E. and Roble, R. G.: Modeling diurnal tidal variability with the National Center for Atmospheric Research thermosphere-ionosphere-mesosphere-electrodynamics general circulation model, *J. Geophys. Res.*, 106, 24 869–24 882, doi:10.1029/2001JA000057, 2001.
- 795 Hagan, M. E., Maute, A., Roble, R. G., Richmond, A. D., Immel, T. J., and England, S. L.: Connections between deep tropical clouds and the Earth's ionosphere, *Geophys. Res. Lett.*, 34, L20109, doi:10.1029/2007GL030142, 2007.
- Häusler, K. and Lühr, H.: Nonmigrating tidal signals in the upper thermospheric zonal wind at equatorial latitudes as observed by CHAMP, *Annales Geophysicae*, 27, 2643–2652, doi:10.5194/angeo-27-2643-2009, 2009.
- Huang, F. T., Mayr, H. G., Reber, C. A., Russell, J. M., Mlynczak, M., and Mengel, J. G.: Stratospheric and mesospheric temperature variations for the quasi-biennial and semiannual (QBO and SAO) oscillations based on measurements from SABER (TIMED) and MLS (UARS), *Ann. Geophys.*, 24, 2131–2149, 2006.
- 800 Immel, T. J., Sagawa, E., England, S. L., Henderson, S. B., Hagan, M. E., Mende, S. B., Frey, H. U., Swenson, C. M., and Paxton, L. J.: Control of equatorial ionospheric morphology by atmospheric tides, *Geophys. Res. Lett.*, 33, L15 108, doi:10.1029/2006GL026161, 2006.
- Jin, H., Miyoshi, Y., Fujiwara, H., and Shinagawa, H.: Electrodynamics of the formation of ionospheric wave number 4 longitudinal structure, *Journal of Geophysical Research (Space Physics)*, 113, A09 307, doi:10.1029/2008JA013301, 2008.
- 805 Kil, H., Oh, S.-J., Kelley, M. C., Paxton, L. J., England, S. L., Talaat, E., Min, K.-W., and Su, S.-Y.: Longitudinal structure of the vertical  $E \times B$  drift and ion density seen from ROCSAT-1, *Geophys. Res. Lett.*, 34, L14 110, doi:10.1029/2007GL030018, 2007.
- Laskar, F. I., Chau, J. L., Stober, G., Hoffmann, P., Hall, C. M., and Tsutsumi, M.: Quasi-biennial oscillation modulation of the middle- and high-latitude mesospheric semidiurnal tides during August-September, *Journal of Geophysical Research (Space Physics)*, 121, 4869–4879, doi:10.1002/2015JA022065, 2016.
- 810 Li, X., Wan, W., Ren, Z., Liu, L., and Ning, B.: The variability of non-migrating tides detected from TIMED/SABER observations, *J. Geophys. Res.*, doi:10.1002/2015JA021577, 2015.
- Lieberman, R. S., Riggin, D. M., Ortlund, D. A., Nesbitt, S. W., and Vincent, R. A.: Variability of mesospheric diurnal tides and tropospheric diurnal heating during 1997-1998, *J. Geophysical Research (Atmospheres)*, 112, D20 110, doi:10.1029/2007JD008578, 2007.
- Lieberman, R. S., Oberheide, J., and Talaat, E. R.: Nonmigrating diurnal tides observed in global thermospheric winds, *J. Geophys. Res. (Space Physics)*, 118, 7384–7397, doi:10.1002/2013JA018975, 2013.
- 815 Lieberman, R. S., Riggin, D. M., Ortlund, D. A., Oberheide, J., and Siskind, D. E.: Global observations and modeling of nonmigrating diurnal tides generated by tide-planetary wave interactions, *J. Geophys. Res.*, doi:10.1002/2015JD023739, 2015.
- Liu, H.-L., Foster, B. T., Hagan, M. E., McInerney, J. M., Maute, A., Qian, L., Richmond, A. D., Roble, R. G., Solomon, S. C., Garcia, R. R., Kinnison, D., Marsh, D. R., Smith, A. K., Richter, J., Sassi, F., and Oberheide, J.: Thermosphere extension of the Whole Atmosphere Community Climate Model, *Journal of Geophysical Research (Space Physics)*, 115, A12 302, doi:10.1029/2010JA015586, 2010.
- 820 Liu, X., Xu, J., Yue, J., Liu, H. L., and Yuan, W.: Large winds and wind shears caused by the nonlinear interactions between gravity waves and tidal backgrounds in the mesosphere and lower thermosphere, *Journal of Geophysical Research*, 119, 7698–7708, doi:10.1002/2014JA020221, 2014.

- Lübken, F.-J., Höffner, J., Viehl, T. P., Kaifler, B., and Morris, R. J.: First measurements of thermal tides in the summer mesopause region at  
825 Antarctic latitudes, *Geophys. Res. Lett.*, 38, L24806, 2011.
- Marsh, D. R., Solomon, S. C., and Reynolds, A. E.: Empirical model of nitric oxide in the lower thermosphere, *Journal of Geophysical Research (Space Physics)*, 109, A07301, doi:10.1029/2003JA010199, 2004.
- Mayr, H. G. and Mengel, J. G.: Interannual variations of the diurnal tide in the mesosphere generated by the quasi-biennial oscillation, *Journal of Geophysical Research*, 110, D10 111, doi:10.1029/2004JD005055, 2005.
- 830 Mayr, H. G., Mengel, J. G., Talaat, E. R., Porter, H. S., and Chan, K. L.: Mesospheric non-migrating tides generated with planetary waves: I. Characteristics, *Journal of Atmospheric and Solar-Terrestrial Physics*, 67, 959–980, doi:10.1016/j.jastp.2005.03.002, 2005a.
- Mayr, H. G., Mengel, J. G., Talaat, E. R., Porter, H. S., and Chan, K. L.: Mesospheric non-migrating tides generated with planetary waves: II. Influence of gravity waves, *Journal of Atmospheric and Solar-Terrestrial Physics*, 67, 981–991, doi:10.1016/j.jastp.2005.03.003, 2005b.
- McLandress, C.: Interannual variations of the diurnal tide in the mesosphere induced by a zonal-mean wind oscillation in the tropics,  
835 *Geophys. Res. Lett.*, 29, 1305, doi:10.1029/2001GL014551, 2002.
- Moudden, Y. and Forbes, J. M.: A decade-long climatology of terdiurnal tides using TIMED/SABER observations, *Journal of Geophysical Research (Space Physics)*, 118, 4534–4550, doi:10.1002/jgra.50273, 2013.
- Mukhtarov, P. and Pancheva, D.: Global ionospheric response to nonmigrating DE3 and DE2 tides forced from below, *Journal of Geophysical Research (Space Physics)*, 116, A05 323, doi:10.1029/2010JA016099, 2011.
- 840 Nee, J. B.: Observations of non-migrating tides and ionospheric perturbations of O(<sup>1</sup>D) airglow by ISUAL instrument, *Advances in Space Research*, 54, 409–416, doi:10.1016/j.asr.2013.09.011, 2014.
- Oberheide, J. and Forbes, J. M.: Tidal propagation of deep tropical cloud signatures into the thermosphere from TIMED observations, *Geophys. Res. Lett.*, 35, L04 816, doi:10.1029/2007GL032397, 2008a.
- Oberheide, J. and Forbes, J. M.: Thermospheric nitric oxide variability induced by nonmigrating tides, *Geophys. Res. Lett.*, 35, L16 814,  
845 doi:10.1029/2008GL034825, 2008b.
- Oberheide, J., Hagan, M. E., Roble, R. G., and Offermann, D.: Sources of nonmigrating tides in the tropical middle atmosphere, *Journal of Geophysical Research (Atmospheres)*, 107, 4567, doi:10.1029/2002JD002220, 2002.
- Oberheide, J., Wu, Q., Ortland, D. A., Killeen, T. L., Hagan, M. E., Roble, R. G., Niciejewski, R. J., and Skinner, W. R.: Non-migrating diurnal tides as measured by the TIMED Doppler interferometer: Preliminary results, *Advances in Space Research*, 35, 1911–1917,  
850 doi:10.1016/j.asr.2005.01.063, 2005.
- Oberheide, J., Wu, Q., Killeen, T. L., Hagan, M. E., and Roble, R. G.: Diurnal nonmigrating tides from TIMED Doppler Interferometer wind data: Monthly climatologies and seasonal variations, *Journal of Geophysical Research (Space Physics)*, 111, A10S03, doi:10.1029/2005JA011491, 2006.
- Oberheide, J., Forbes, J. M., Häusler, K., Wu, Q., and Bruinsma, S. L.: Tropospheric tides from 80 to 400 km: Propagation, interannual  
855 variability, and solar cycle effects, *J. Geophys. Res.*, 114, D00I05, doi:10.1029/2009JD012388, 2009.
- Oberheide, J., Forbes, J. M., Zhang, X., and Bruinsma, S. L.: Wave-driven variability in the ionosphere-thermosphere-mesosphere system from TIMED observations: What contributes to the wave 4?, *Journal of Geophysical Research*, 116, A01306, doi:10.1029/2010JA015911, 2011a.
- Oberheide, J., Forbes, J. M., Zhang, X., and Bruinsma, S. L.: Climatology of upward propagating diurnal and semidiurnal tides in the  
860 thermosphere, *Journal of Geophysical Research (Space Physics)*, 116, A11 306, doi:10.1029/2011JA016784, 2011b.

- Oberheide, J., Mlynczak, M. G., Mosso, C. N., Schroeder, B. M., Funke, B., and Maute, A.: Impact of tropospheric tides on the nitric oxide 5.3  $\mu\text{m}$  infrared cooling of the low-latitude thermosphere during solar minimum conditions, *J. Geophys. Res.*, 118, doi:10.1002/2013JA019278, <http://dx.doi.org/10.1002/2013JA019278>, 2013.
- Oelhaf, H.: MIPAS Mission Plan, ESA Technical Note ENVI-SPPA-EOPG-TN-07-0073, 2008.
- 865 Pancheva, D. and Mukhtarov, P.: Strong evidence for the tidal control on the longitudinal structure of the ionospheric F-region, *Geophys. Res. Lett.*, 37, L14 105, doi:10.1029/2010GL044039, 2010.
- Pancheva, D. and Mukhtarov, P.: *Aeronomy of the Earth's Atmosphere and Ionosphere*, chap. 2. Atmospheric Tides and Planetary Waves: Recent Progress Based on SABER/TIMED Temperature Measurements (2002–2007), pp. 19–56, IAGA Special Sopron Book Series 2, Springer, Ed. by M.A. Abdu, D. Pancheva, A. Bhattacharyya, doi:10.1007/978-94-007-0326-1\_2, 2011.
- 870 Pancheva, D., Mukhtarov, P., and Andonov, B.: Global structure, seasonal and interannual variability of the eastward propagating tides seen in the SABER/TIMED temperatures (2002–2007), *Advances in Space Research*, 46, 257–274, doi:10.1016/j.asr.2010.03.026, 2010.
- Pancheva, D., Mukhtarov, P., and Smith, A. K.: Climatology of the migrating terdiurnal tide (TW3) in SABER/TIMED temperatures, *Journal of Geophysical Research (Space Physics)*, 118, 1755–1767, doi:10.1002/jgra.50207, 2013.
- Pedatella, N. M. and Liu, H.-L.: Tidal variability in the mesosphere and lower thermosphere due to the El Niño–Southern Oscillation, 875 *Geophys. Res. Lett.*, 39, L19802, doi:10.1029/2012GL053383, 2012.
- Pedatella, N. M., Forbes, J. M., and Oberheide, J.: Intra-annual variability of the low-latitude ionosphere due to nonmigrating tides, *Geophys. Res. Lett.*, 35, L18 104, doi:10.1029/2008GL035332, 2008.
- Pedatella, N. M., Hagan, M. E., and Maute, A.: The comparative importance of DE3, SE2, and SPW4 on the generation of wavenumber-4 longitude structures in the low-latitude ionosphere during September equinox, *Geophys. Res. Lett.*, 39, L19 108, doi:10.1029/2012GL053643, 880 2012.
- Picone, J., Hedin, A., Drob, D., and Aikin, A.: NRLMSISE-00 empirical model of the atmosphere: Statistical comparisons and scientific issues, *J. Geophys. Res.*, 107, 1468, doi:10.1029/2002JA009 430, 2002.
- Ribstein, B., Achatz, U., and Senf, F.: The interaction between gravity waves and solar tides: Results from 4-D ray tracing coupled to a linear tidal model, *Journal of Geophysical Research*, 120, 6795–6817, doi:10.1002/2015JA021349, 2015.
- 885 Scherliess, L., Thompson, D. C., and Schunk, R. W.: Longitudinal variability of low-latitude total electron content: Tidal influences, *Journal of Geophysical Research (Space Physics)*, 113, A01 311, doi:10.1029/2007JA012480, 2008.
- Senf, F. and Achatz, U.: On the impact of middle-atmosphere thermal tides on the propagation and dissipation of gravity waves, *Journal of Geophysical Research (Atmospheres)*, 116, D24110, doi:10.1029/2011JD015794, 2011.
- Shepherd, G. G.: Thermospheric observations of equatorial wavenumber 4 density perturbations from WINDII data, *Geophys. Res. Lett.*, 38, 890 L08 801, doi:10.1029/2011GL046986, 2011.
- Shepherd, M. G., Shepherd, G. G., and Cho, Y.-M.: Longitudinal variability of thermospheric temperatures from WINDII O(<sup>1</sup>S) dayglow, *Journal of Geophysical Research (Space Physics)*, 117, A10 302, doi:10.1029/2012JA017777, 2012.
- Smith, A. K., Marsh, D. R., and Szymczak, A. C.: Interaction of chemical heating and the diurnal tide in the mesosphere, *Journal of Geophysical Research (Atmospheres)*, 108, 4164, doi:10.1029/2002JD002664, 2003.
- 895 Talaat, E. R. and Lieberman, R. S.: Direct observations of nonmigrating diurnal tides in the equatorial thermosphere, *Geophys. Res. Lett.*, 37, L04 803, doi:10.1029/2009GL041845, 2010.
- Teitelbaum, H. and Vial, F.: On tidal variability induced by nonlinear interaction with planetary waves, *J. Geophys. Res.*, 96, 14, doi:10.1029/91JA01019, 1991.

- Thayaparan, T.: The terdiurnal tide in the mesosphere and lower thermosphere over London, Canada (43°N, 81°W), *J. Geophys. Res.*, 102, 21, doi:10.1029/97JD01839, 1997.
- Truskowski, A. O., Forbes, J. M., Zhang, X., and Palo, S. E.: New perspectives on thermosphere tides: 1. Lower thermosphere spectra and seasonal-latitude structures, *Earth, Planets, and Space*, 66, 136, doi:10.1186/s40623-014-0136-4, 2014.
- von Clarmann, T., Höpfner, M., Kellmann, S., Linden, A., Chauhan, S., Grabowski, U., Funke, B., Glatthor, N., Kiefer, M., Schieferdecker, T., and Stiller, G. P.: Retrieval of temperature H<sub>2</sub>O, O<sub>3</sub>, HNO<sub>3</sub>, CH<sub>4</sub>, N<sub>2</sub>O and ClONO<sub>2</sub> from MIPAS reduced resolution nominal mode limb emission measurements, *Atmos. Meas. Tech.*, 2, 159–175, <http://www.atmos-meas-tech.net/2/159/2009/>, 2009.
- Wang, D. Y., Ward, W. E., Shepherd, G. G., and Wu, D.-L.: Stationary Planetary Waves Inferred from WINDII Wind Data Taken within Altitudes 90–120 km during 1991–96, *J. Atmos. Sci.*, 57, 1906–1918, 2000.
- Ward, W. E., Fomichev, V. I., and Beagley, S.: Nonmigrating tides in equinox temperature fields from the Extended Canadian Middle Atmosphere Model (CMAM), *Geophys. Res. Lett.*, 32, L03803, doi:10.1029/2004GL021466, 2005.
- Williams, C. R. and Avery, S. K.: Diurnal nonmigrating tidal oscillations forced by deep convective clouds, *J. Geophys. Res.*, 101, 4079–4091, doi:10.1029/95JD03007, 1996.
- Wu, Q., Ortland, D. A., Solomon, S. C., Skinner, W. R., and Niciejewski, R. J.: Global distribution, seasonal, and inter-annual variations of mesospheric semidiurnal tide observed by TIMED TIDI, *Journal of Atmospheric and Solar-Terrestrial Physics*, 73, 2482–2502, doi:10.1016/j.jastp.2011.08.007, 2011.
- Xu, J., Smith, A. K., Liu, H.-L., Yuan, W., Wu, Q., Jiang, G., Mlynczak, M. G., Russell, J. M., and Franke, S. J.: Seasonal and quasi-biennial variations in the migrating diurnal tide observed by Thermosphere, Ionosphere, Mesosphere, Energetics and Dynamics (TIMED), *J. Geophys. Res.*, 114, 13 107, doi:10.1029/2008JD011298, 2009.
- Xu, J., Smith, A. K., Wang, W., Jiang, G., Yuan, W., Gao, H., Yue, J., Funke, B., López-Puertas, M., and Russell, J. M.: An observational and theoretical study of the longitudinal variation in neutral temperature induced by aurora heating in the lower thermosphere, *J. Geophys. Res.*, 118, 7410–7425, doi:10.1002/2013JA019144, <http://dx.doi.org/10.1002/2013JA019144>, 2013.
- Yue, J., Xu, J., Chang, L. C., Wu, Q., Liu, H.-L., Lu, X., and Russell, J.: Global structure and seasonal variability of the migrating terdiurnal tide in the mesosphere and lower thermosphere, *J. Atmos. Sol.-Terr. Phys.*, 105, 191–198, doi:10.1016/j.jastp.2013.10.010, 2013.
- Zhang, L., Jakob, D. J., Bowman, K. W., Logan, J. A., Turquety, S., Hudman, R. C., Li, Q., Beer, R., Worden, H. M., Worden, J. R., Rinsland, C. P., Kulawik, S. S., Lampel, M. C., Shephard, M. W., Fisher, B. M., Eldering, A., and Avery, M. A.: Ozon–CO correlations determined by the TES satellite instrument in continental outflow regions, *Geophys. Res. Lett.*, 33, L18804, doi:10.1029/2006GL026399, 2006.
- Zhang, X., Forbes, J. M., Hagan, M. E., Russell, J. M., Palo, S. E., Mertens, C. J., and Mlynczak, M. G.: Monthly tidal temperatures 20–120 km from TIMED/SABER, *J. Geophys. Res.*, 111, 10, doi:10.1029/2005JA011504, 2006.
- Zhang, X., Forbes, J. M., and Hagan, M. E.: Longitudinal variation of tides in the MLT region: 1. Tides driven by tropospheric net radiative heating, *Journal of Geophysical Research (Space Physics)*, 115, A06 316, doi:10.1029/2009JA014897, 2010a.
- Zhang, X., Forbes, J. M., and Hagan, M. E.: Longitudinal variation of tides in the MLT region: 2. Relative effects of solar radiative and latent heating, *Journal of Geophysical Research (Space Physics)*, 115, A06 317, doi:10.1029/2009JA014898, 2010b.
- Zhu, X., Yee, J.-H., Talaat, E. R., Mlynczak, M., Gordley, L., Mertens, C., and Russell III, J. M.: An algorithm for extracting zonal mean and migrating tidal fields in the middle atmosphere from satellite measurements: Applications to TIMED/SABER–measured temperature and tidal modeling, *J. Geophys. Res.*, 110, D02105, doi:10.1029/2004JD004996, 2005.

**Table 1.** Main tidal component contributions resolved in our spectral analysis. The derived amplitudes and phases are a combination of all modes contributing.

n	wavenumber $ n - s $	components
odd	0	DW1+TW3
	1	D0+DW2+TW2
	2	DW3+DE1+TW1
	3	DE2+DW4+T0
	4	DE3+DW5+TE1

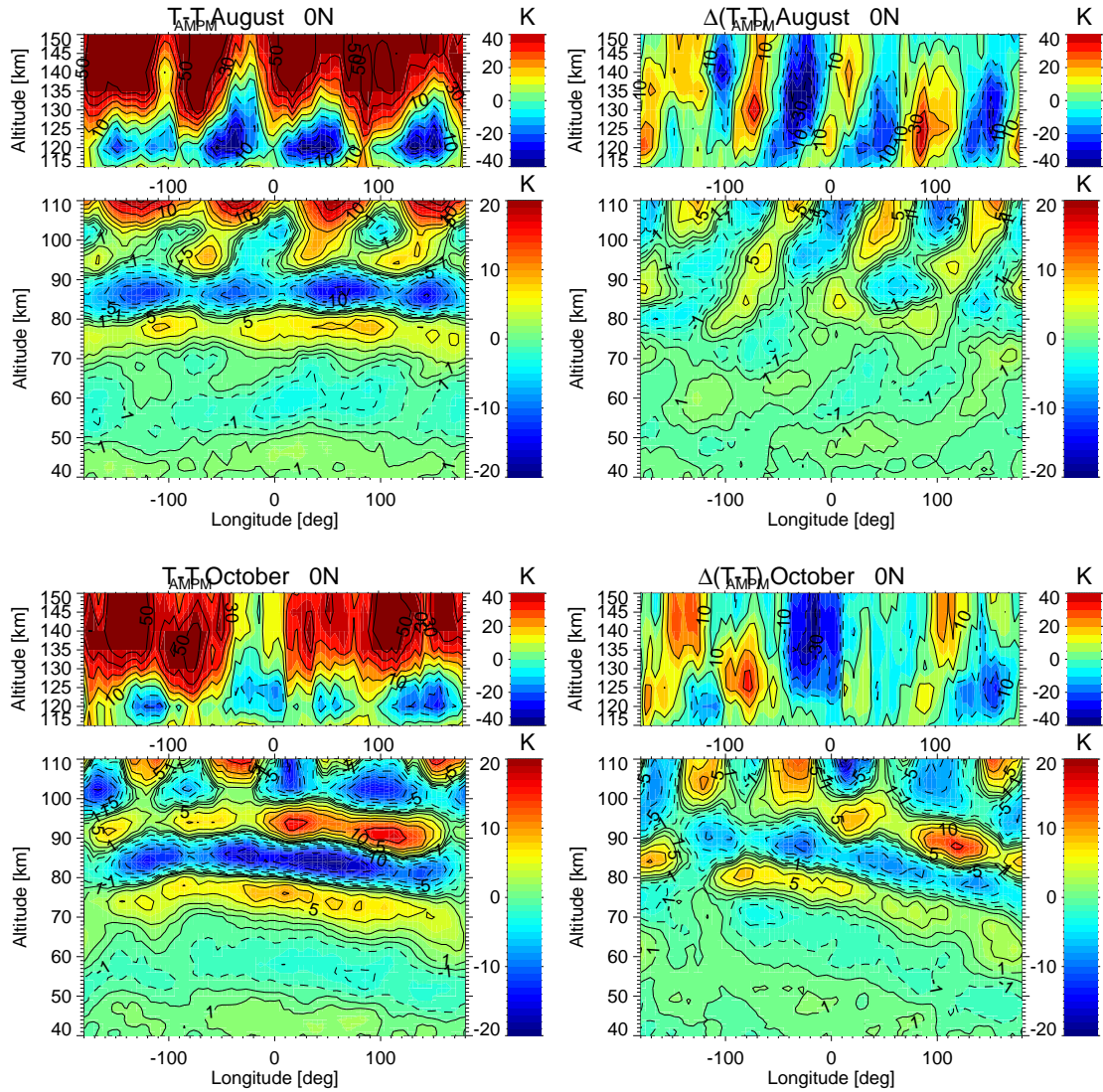


**Figure 1.** Equatorial MIPAS monthly mean temperature difference (left) and anomaly (with respect to the mean value at each altitude; right) of  $\Delta T/2$  for August (1<sup>st</sup> and 2<sup>nd</sup> rows) and October (3<sup>rd</sup> and 4<sup>th</sup> rows) averaged for 2007-2012. Temperatures below 110 km are retrieved from measurements at 15  $\mu\text{m}$  and above 115 km from 5.3  $\mu\text{m}$ . Note the different color scales.

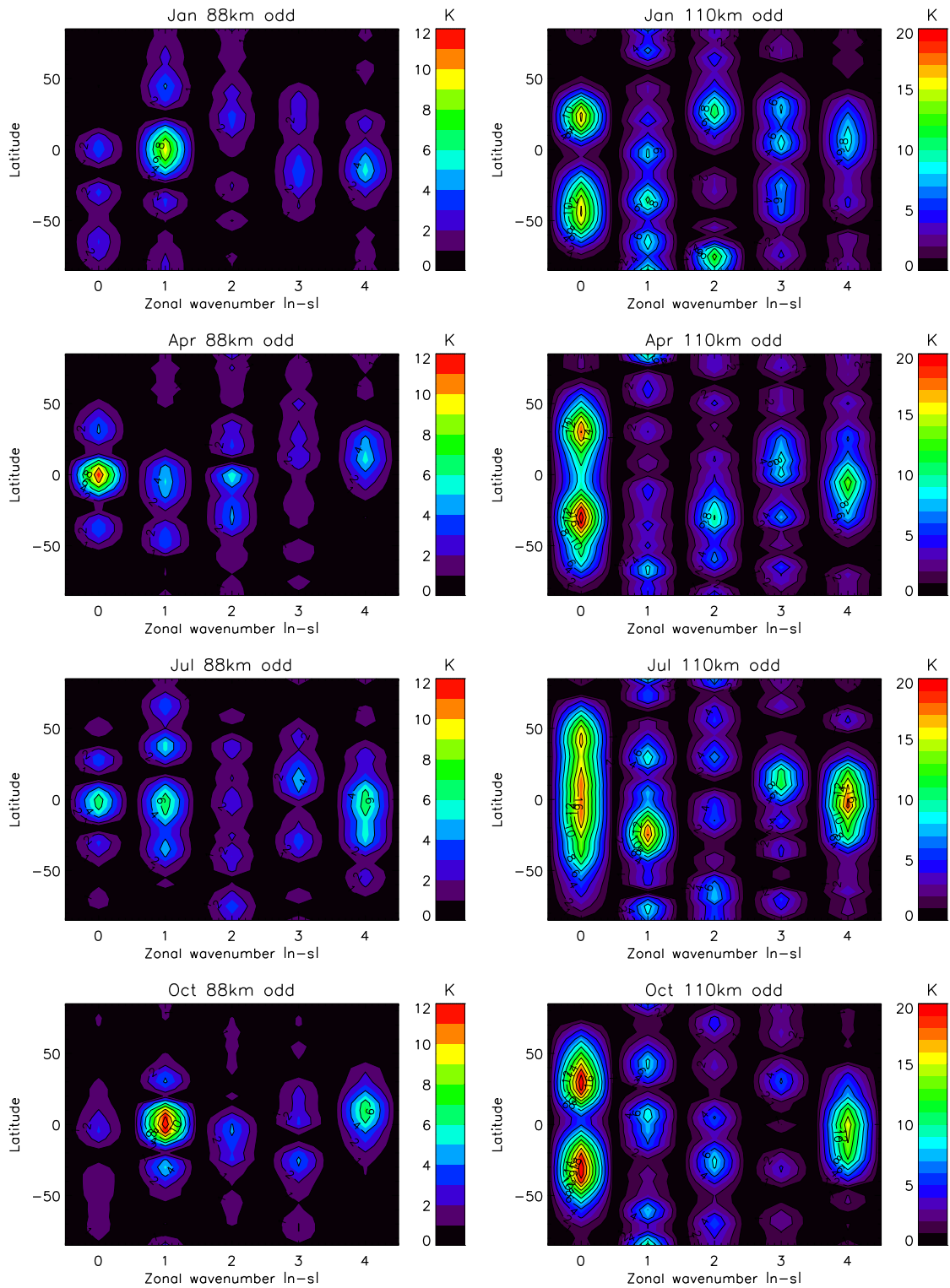


**Figure 2.** MIPAS  $\Delta T/2$  average (2007-2012) monthly mean spectra at 88 km (left) and 110 km (right) for January (1<sup>st</sup> row), April (2<sup>nd</sup>

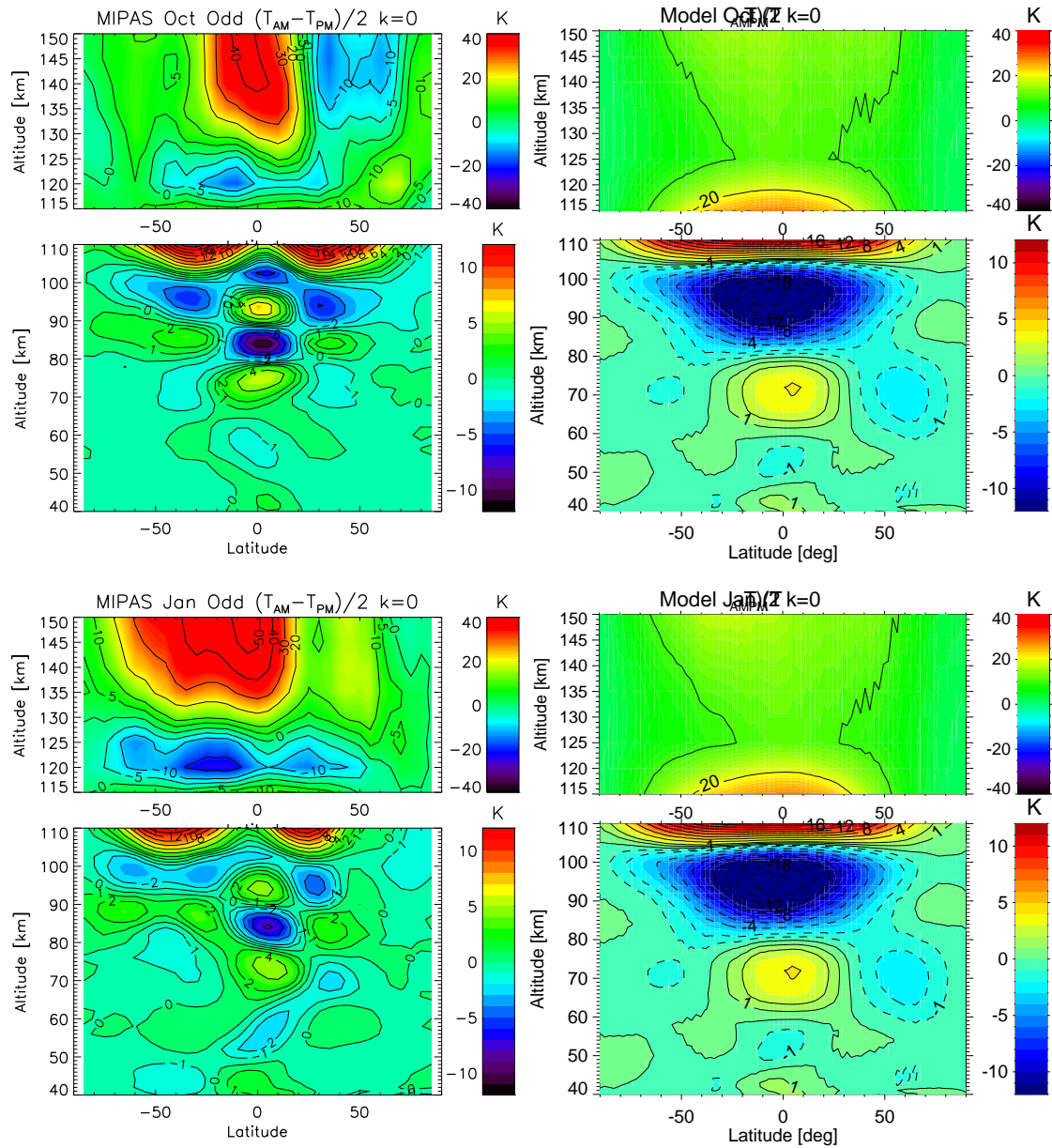


**Figure 3.** Zonal means of  $\Delta T/2$  ( $|n_{odd} - s|=0$  mode, embedding DW1 and TW3) extracted from average (2007-2012) monthly means of MIPAS  $T_{MLT}$  (20-110 km) and  $T_{THER}$  (115-150 km) temperatures (left) compared to results for ~~DW1 from GSWM~~ ECMWF and NRLMSISE-00, respectively (see text) (right), for October (1<sup>st</sup> and 2<sup>nd</sup> rows) and January (3<sup>rd</sup> and 4<sup>th</sup> rows).

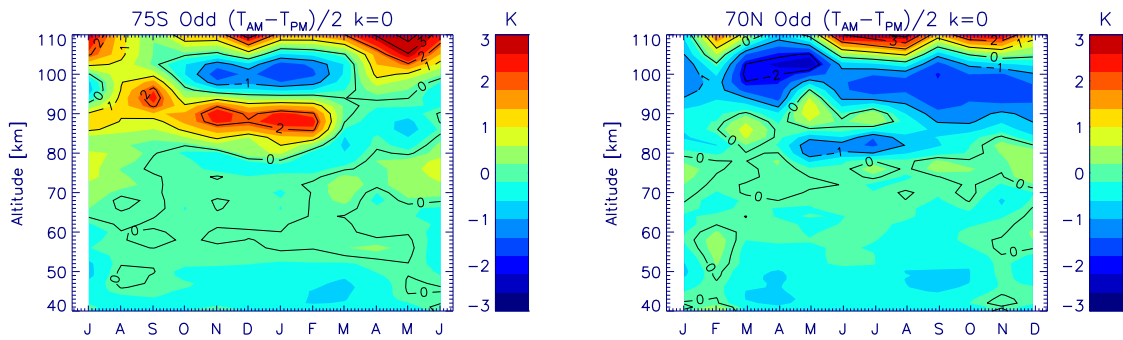


**Figure 4.** Time series of the vertical distribution of average (2007-2012)  $\Delta T/2$  monthly zonal means ( $|n_{odd} - s|=0$  mode) at high latitudes ( $75^\circ\text{S}$ , left;  $75^\circ\text{N}$ , right).

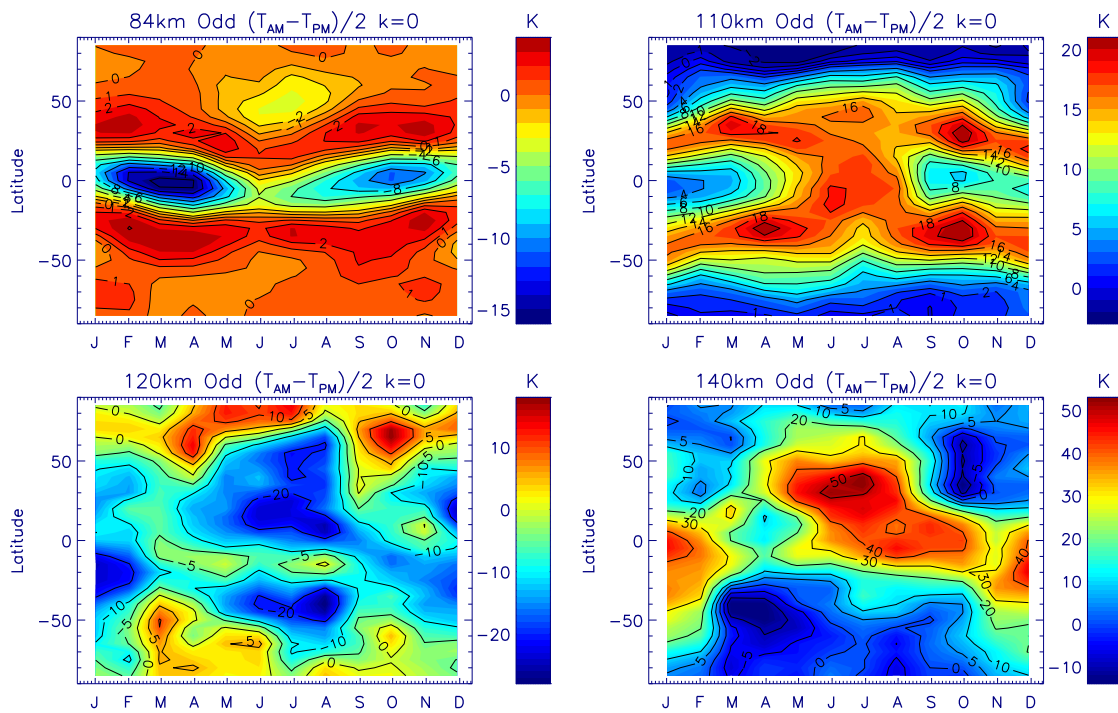


**Figure 5.** Time series of the latitudinal distribution of average (2007-2012) monthly zonal mean  $\Delta T/2$  ( $|n_{odd} - s|=0$  mode) at 84, 110, 120 and 140 km.

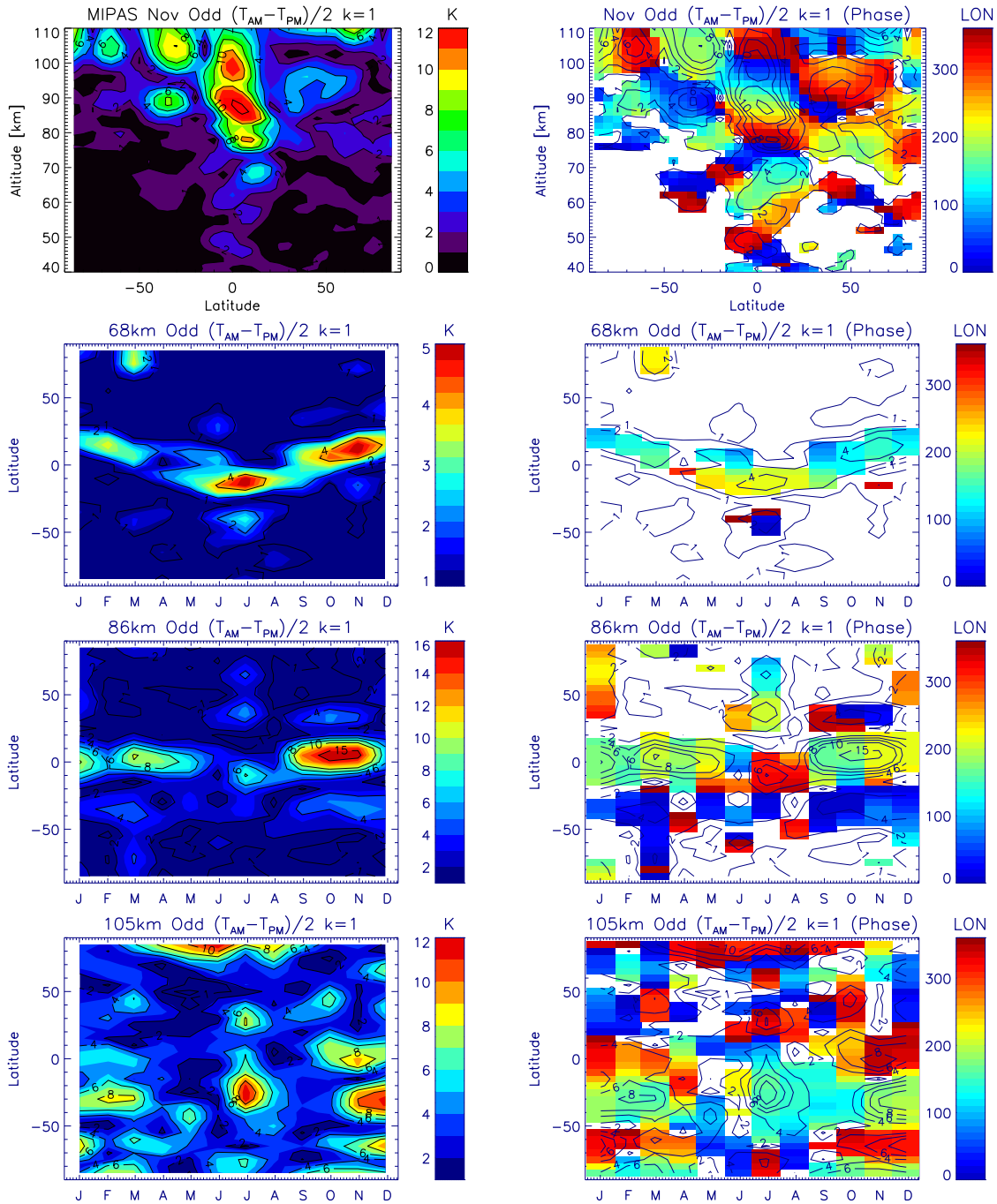


**Figure 6.** Latitude-altitude fields for November (1<sup>st</sup> row) and latitude-time fields at 68, 86 and 105 km (2<sup>nd</sup>-4<sup>th</sup> rows) of amplitudes and phases of MIPAS average (2007-2012)  $|n_{odd} - s|=1$  mode. It embeds D0, DW2 and TW2 tidal oscillations.

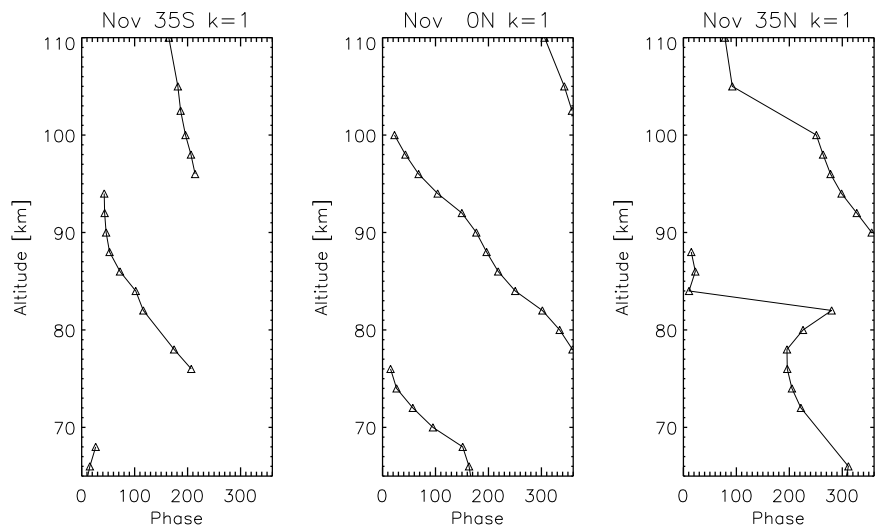


**Figure 7.** Phase of MIPAS average (2007-2012)  $|n_{odd} - s|=1$  for November at  $35^{\circ}\text{S}$  (left), equator (center) and  $35^{\circ}\text{N}$  (right).

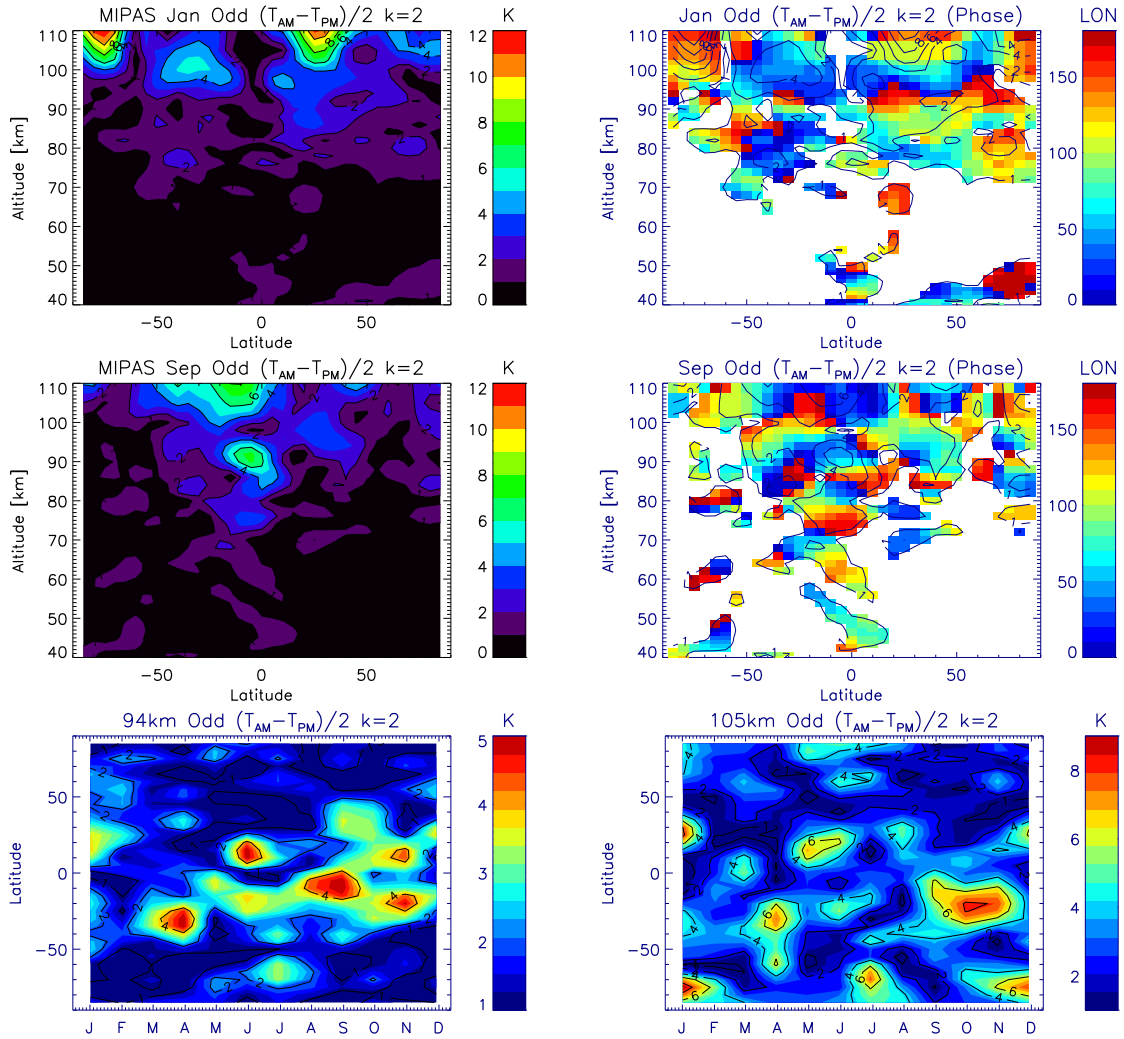


**Figure 8.** Latitude-altitude amplitude (left) and phase (right) fields for January (1<sup>st</sup> row) and September (2<sup>nd</sup> row) and latitude-time horizontal slices of amplitudes (3<sup>rd</sup> row) at 94 km (left) and 105 km (right) of MIPAS average (2007-2012)  $|n_{odd} - s| = 2$  mode. It comprises effects from the DW3, DE1 and TW1 tidal modes.

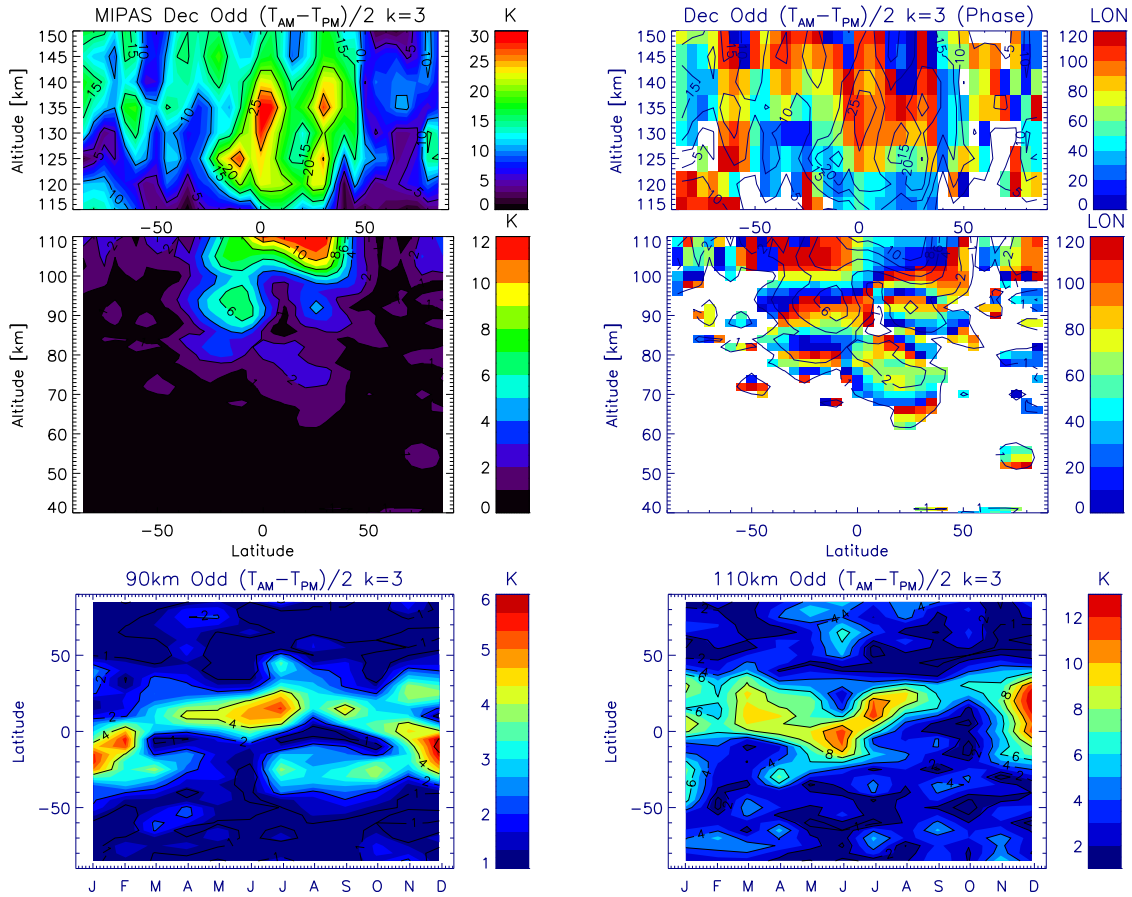


**Figure 9.** Latitude-altitude amplitude (left) and phase (right) fields for December MIPAS average (2007-2012)  $|n_{odd} - s|=3$  longitudinal oscillations (1<sup>st</sup> and 2<sup>nd</sup> row) and average monthly mean time series of  $|n_{odd} - s|=3$  amplitudes at 90 km (left) and 110 km (right). They embed [contribution-contributions](#) from [DW3DE2](#), [DE1-DW4](#) and [TW1-T0](#) tides.

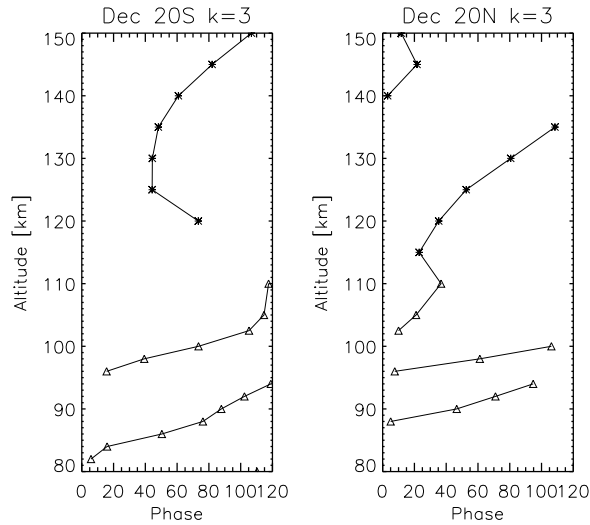


**Figure 10.** Phase of MIPAS average (2007-2012)  $|n_{odd} - s|=3$  for December at 20°S (left) and 20°N (right).

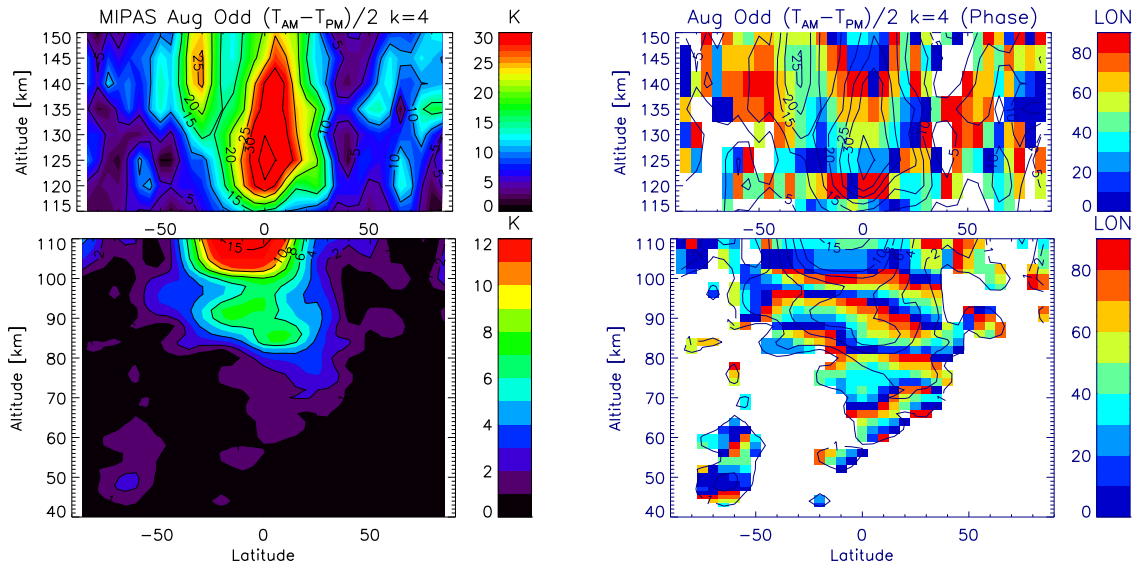


**Figure 11.** August average (2007-2012) monthly mean amplitudes (left) and phases (right)  $|n_{odd} - s|=4$  oscillations from MIPAS  $T_{THER}$  (115-150 km; upper panels) and  $T_{MLT}$  (20-110 km; bottom panels) temperatures. Note the different color scale. They embed the DE3 and TE1 tides.

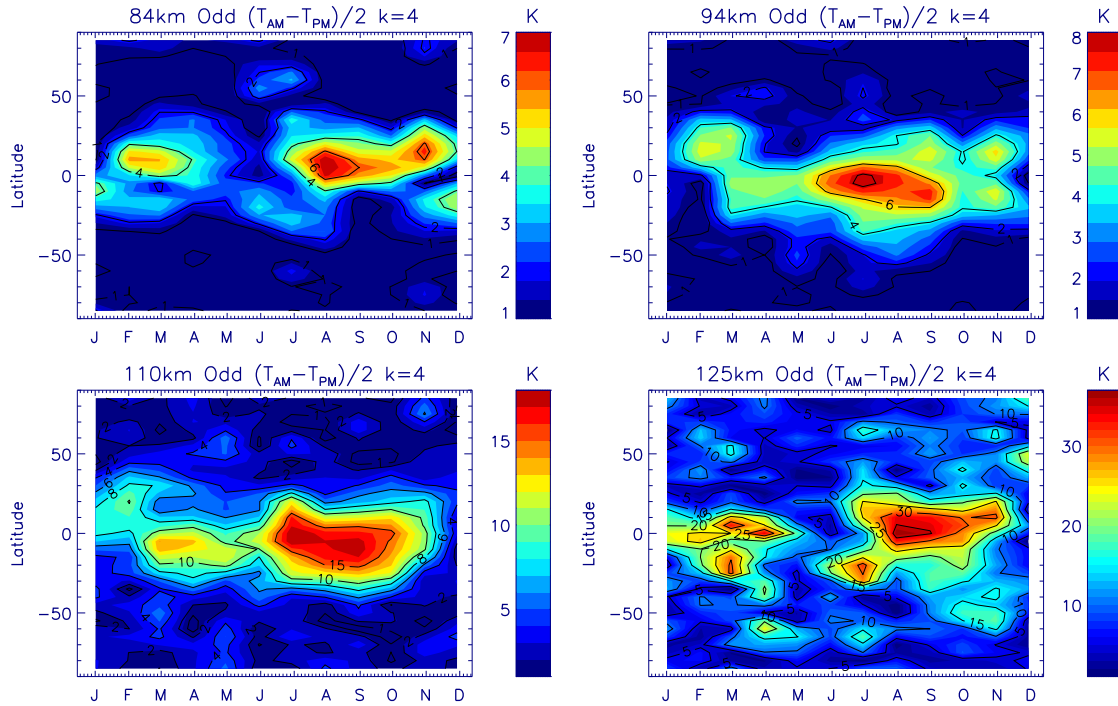


**Figure 12.** Time series of latitudinal distribution of average (2007-2012) monthly means amplitudes for the MIPAS  $|n_{odd} - s|=4$  mode at 84, 94, 110 and 125 km. It embeds DE3 and TE1 tidal oscillations.

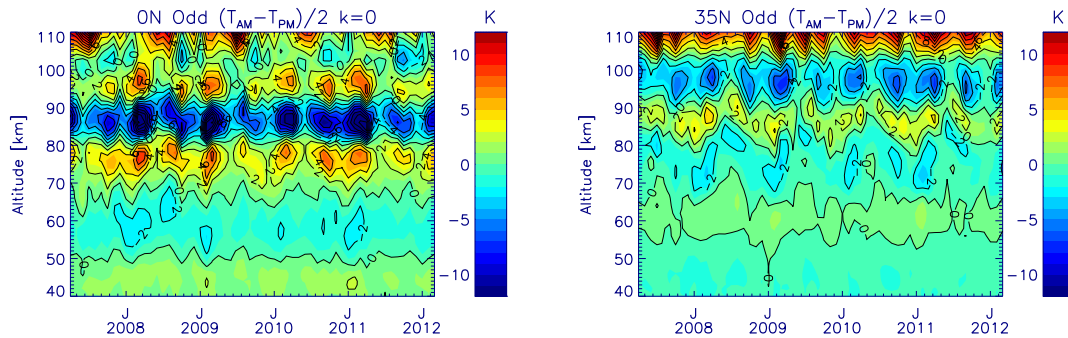


**Figure 13.** Time series of the MIPAS zonal mean of  $\Delta T/2$  monthly means ( $|n_{odd} - s|=0$  mode) at the equator (left) and over 35°N (right).

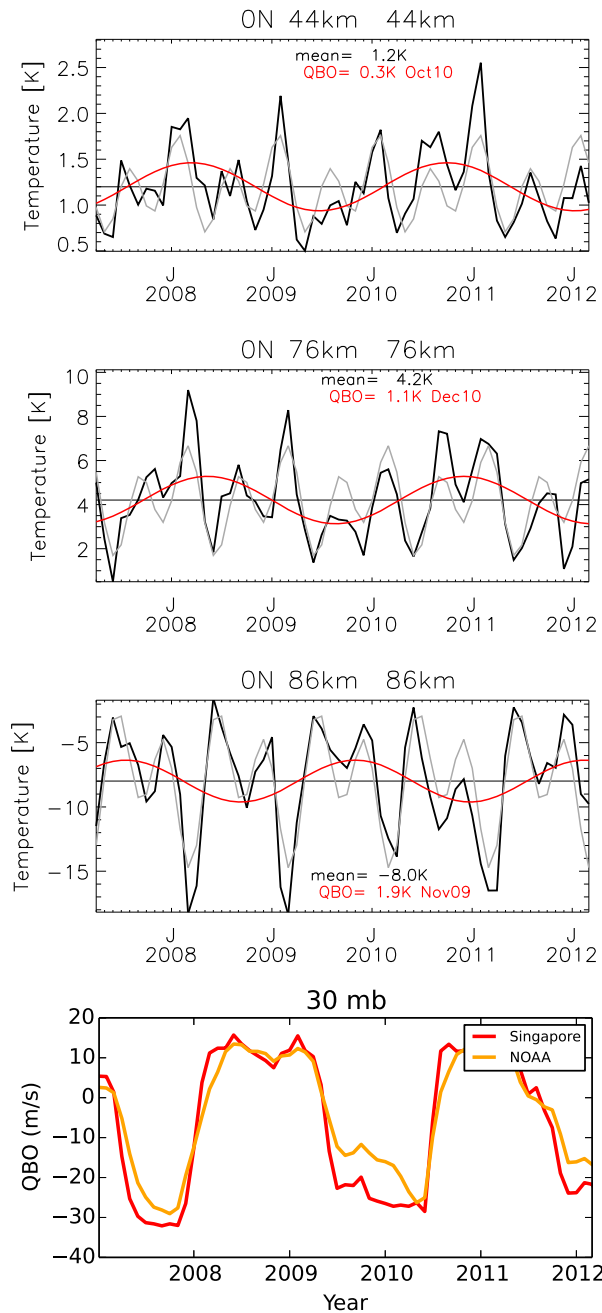


**Figure 14.** MIPAS monthly mean  $|n_{odd} - s|=0$  mode perturbations (black lines) at 44, 76 and 86 km and their decomposition in annual plus semi-annual components (blue) and QBO (red). Singapore winds at 30 mb are also plotted in the bottom panel for reference.

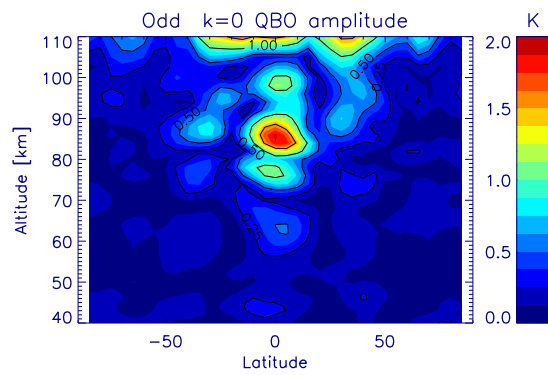


**Figure 15.** QBO amplitudes derived from the MIPAS  $|n_{odd} - s|=0$  longitudinal mode extracted from monthly means from April 2007 to March 2012.